Electronic Supplementary Information (ESI)

Zwitterionic dioxidovanadium(v) complexes containing fluorinated triphenylphosphonium ligands: Structure and biomacromolecules studies

Francisco Mainardi Martins,[a] Daniele Cocco Durigon,[b] Otávio Augusto Chaves,[d] Rosely A. Peralta,[c] Davi Fernando Back[a]* and Hernán Terenzi[b*]

[a]*Laboratory of Inorganic Materials, Department of Chemistry, CCNE, Federal University of Santa Maria, Santa Maria – RS – Brazil, 97105-900.*

[b]*Laboratory of Structural Molecular Biology, Department of Biochemistry, Federal University of Santa Catarina, Florianópolis – SC – Brazil, 88040-900.*

[c]*Laboratory of Bioinorganic and Crystallography, Department of Chemistry, Federal University of Santa Catarina, Florianópolis – SC – Brazil, 88040-900.*

[d]*CQC-IMS, Department of Chemistry, University of Coimbra, Coimbra – Portugal, 3004-535.*

*Corresponding authors:

e-mail: davi.f.back@ufsm.br. (D. F. Back).

e-mail: hernan.terenzi@ufsc.br. (H. Terenzi).

Electronic Supplementary Information caption

S1 Synthesis procedures and spectroscopic data of 5-(chloromethyl)-2-hydroxybenzaldehyde, **[AF]Cl**, **[H_2L1]Cl**–**[H_3L3]Cl,** and **C1**–**C3**

S1.1 5-(chloromethyl)-2-hydroxybenzaldehyde

For this synthesis, an experimental procedure already published was used[1]. In a 250 mL round bottom flask, 8 g of paraformaldehyde and 60 mL of hydrochloric acid were added. Under constant magnetic stirring, 150 mmol of salicylaldehyde (18.32 g; 15.65 mL) and a few drops of sulfuric acid were added. This reaction mixture was maintained under constant magnetic stirring and under heating in an oil bath at 50 °C for 48 hours (**Scheme S1**).

After, the solid formed was separated by filtration and the solid was washed with 200 mL of deionized water and the solid was solubilized with dichloromethane. After filtration and evaporation of the solvent at room temperature, a light beige solid was obtained. The purity of the compound was sufficient to proceed to the following reactions.

(23.30 g, 91.1 %). mp 79 °C (from MeCN/CH_2Cl_2). ν_{max}/cm^{-1} (FT-IR) 3209br (OH), 3069w $(C–H)_{aromatic}$, 2966w $(C–H)_{aliphatic}$, and 1650s (C=O). ν_{max}/cm^{-1} (FT-Raman) 3071w $(C–H)_{aromatic}$, 2967w $(C–H)_{aliphatic}$, and 1651s (C=O). δ_H(600 MHz; $CDCl_3$; Me_4Si) 4.58 (2 H, s, CH_2), 6.97, 6.98 (1 H, d, $CH_{aromatic}$), 7.53–7.55 (1 H, m, $CH_{aromatic}$), 7.57, 7.57 (1 H, d, $CH_{aromatic}$), 9.87 (1 H, s, $CH_{aldehyde}$), and 11.05 (1 H, s, OH). δ_C(151 MHz; $CDCl_3$; Me_4Si) 45.24, 118.28, 120.33, 129.21, 133.64, 137.31, and 161.57.

S1.2 (3-formyl-4-hydroxybenzyl)tris(4-fluorophenyl)phosphonium chloride (**[AF]Cl**)

For this synthesis, an experimental procedure already published was used, but using tris(4-fluorophenyl)phosphine[1]. This reaction was carried out in a system under an inert atmosphere of argon. In a 100 mL round bottom flask, 2.00 mmol of 5-(chloromethyl)-2-hydroxybenzaldehyde (0.340 g) was dissolved in 10 mL of toluene. Under magnetic stirring and heating in an oil bath at 80 °C, 2.20 mmol of tris(4-fluorophenyl)phosphine (0.696 g) dissolved in 20 mL of toluene was added via a dropping funnel. The reaction system was heated to 100 °C and the conditions of temperature, stirring and inert atmosphere were maintained for 6 hours (**Scheme S1**). After, a greenish yellow solid was separated by filtration and purified by washing with 30 mL of hot toluene and 5 mL of diethyl ether and dried at open atmosphere.

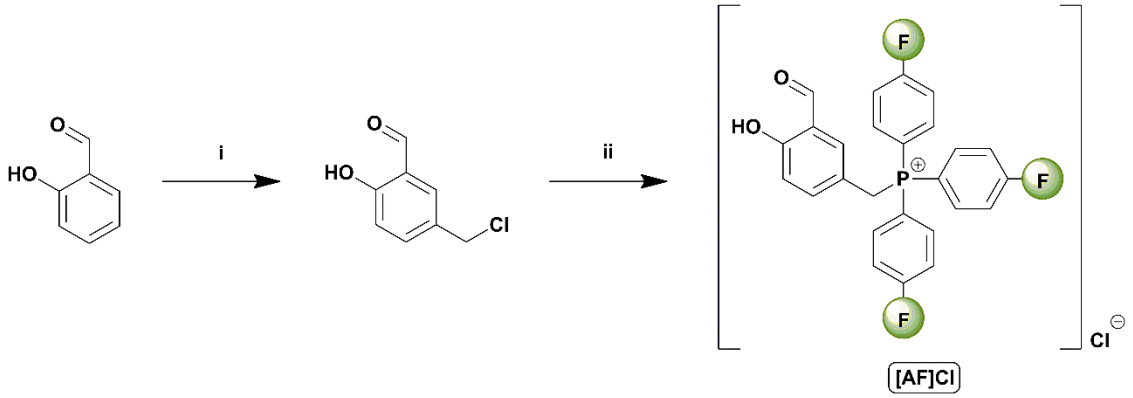

i = Hydrochloric acid, paraformaldehyde, sulfuric acid, 50°C, 48 hours
ii = Argon, toluene, tris(4-fluorophenyl)phosphine, 100°C, 6 hours

Scheme S1 Synthesis of 5-(chloromethyl)-2-hydroxybenzaldehyde and **[AF]Cl**.

(0.853 g, 87.6 %). mp 212 °C. ν_{max}/cm^{-1} (FT-IR) 3043w $(C–H)_{aromatic}$, 2977w $(C–H)_{aliphatic}$, and 1674s (C=O). δ_H(600 MHz; DMSO-d_6) 5.21, 5.24 (2 H, d, CH_2), 7.07–7.10 (1 H, m, $CH_{aromatic}$), 7.13–7.14 (1 H, m, $CH_{aromatic}$), 7.16–7.17 (1 H, m, $CH_{aromatic}$), 7.62–7.65 (6 H, m, $CH_{aromatic}$), 7.78–7.82 (6 H, m, $CH_{aromatic}$), 10.17 (1 H, s, $CH_{aldehyde}$), and 11.34 (1 H, s, OH). δ_C(151 MHz; DMSO-d_6) 27.56, 27.87, 113.47, 113.49, 114.06, 114.09, 117.53, 117.57, 117.62, 117.65, 117.74, 117.80, 117.89, 118.20, 118.22, 122.52, 122.54, 130.22, 130.26, 137.39, 137.46, 137.53, 137.94, 137.97, 161.07, 161.08, 165.24, 165.27, 166.94, 166.96, and 189,36. δ^{19}_F(565 MHz; DMSO-d_6) -101.91. δ^{31}_P(243 MHz; DMSO-d_6; PPh_3) 21.39.

S1.3 Synthesis and spectroscopic data of the ligands **[H$_2$L1]Cl**–**[H$_3$L3]Cl**

In a 50 mL round bottom flask, 0.30 mmol of (3-formyl-4-hydroxybenzyl)tris(4-fluorophenyl)phosphonium chloride (**[AF]Cl**, 0.146 g) and 0.30 mmol of the respective hydrazide (**[H$_2$L1]Cl**: nicotinic, 0.041 g; **[H$_2$L2]Cl**: isonicotinic, 0.041 g, and **[H$_3$L3]Cl**: 3-hydroxy-2-naphthoic, 0.061 g) were solubilized in 20 mL of ethanol. The mixture was maintained under constant magnetic stirring and heating in an oil bath at 90°C for 6 hours (**Scheme S2**).

After, the resulting yellow mixture was added to small vials. After evaporation of ethanol, the ligands were purified by silica gel column chromatography with a mixture (v/v) 85:15 (**[H$_2$L1]Cl**) or 90:10 (**[H$_2$L2]Cl** and **[H$_3$L3]Cl**) dichloromethane/methanol as eluent. **[H$_2$L1]Cl** and **[H$_2$L2]Cl** were washed with 5 mL of diethyl ether and 2 mL of deionized water, while **[H$_3$L3]Cl** was washed only with with 5 mL of diethyl ether. The compounds were dried at 50 °C for 24 hours.

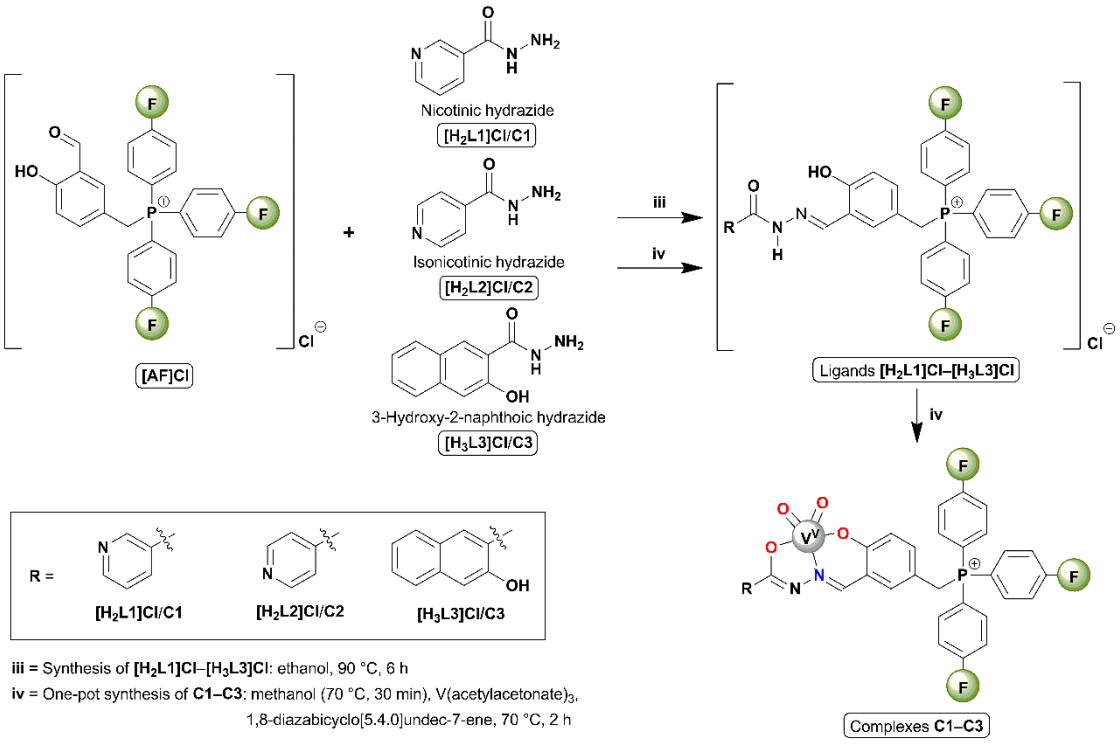

Scheme S2 General synthesis of ligands **[H$_2$L1]Cl**–**[H$_3$L3]Cl** and complexes **C1**–**C3.**

S1.3.1 Ligand {(*E*)-{4-hydroxy-3-[(2-nicotinoylhydrazono)methyl]benzyl}tris(4-fluorophenyl)phosphonium chloride (**[H_2L1]Cl**)

(0.102 g, 56.1 % after purification). mp 172 °C. ν_{max}/cm^{-1} (FT-IR) 3389br (O–H), 3030w $(C–H)_{aromatic}$, 2970w $(C–H)_{aliphatic}$, 1665s (C=O), and 1625w (C=N). δ_H(600 MHz; DMSO-d_6) 5.17, 5.20 (2 H, d, CH_2), 6.89 (2 H, s, $CH_{aromatic}$), 7.28 (1 H, s, $CH_{aromatic}$), 7.57–7.61 (2 H, m, $CH_{aromatic}$), 7.63–7.65 (6 H, t, $CH_{aromatic}$), 7.77–7.81 (6 H, m, $CH_{aromatic}$), 8.38, 8.39 (1 H, d, $CH_{aromatic}$), 8.69 (1 H, s, N=CH), 9.18 (1 H, s, $CH_{aromatic}$), 11.32 (1 H, s, OH), and 12.66 (1 H, s, NH). δ_C(151 MHz; DMSO-d_6) 27.80, 28.11, 113.61, 113.62, 114.20, 114.22, 117.10, 117.12, 117.71, 117.80, 117.86, 117.95, 119.55, 119.57, 131.02, 131.05, 133.34, 133.37, 135.56, 137.39, 137.46, 137.53, 146.80, 148.87, 152.45, 157.35, 157.37, 161.38, 165.27, 165.29, 166.97, and 166.99. δ^{19}_F(565 MHz; DMSO-d_6; $PhCF_3$) -101.83. δ^{31}_P(243 MHz; DMSO-d_6; PPh_3) 21.14.

S1.3.2 Ligand {(*E*)-{4-hydroxy-3-[(2-isonicotinoylhydrazono)methyl]benzyl}tris(4-fluorophenyl)phosphonium chloride (**[H_2L2]Cl**)

(0.075 g, 41.3 % after purification). mp 182 °C (decomposition). ν_{max}/cm^{-1} (FT-IR) 3399br (O–H), 3033w $(C–H)_{aromatic}$, 2956w $(C–H)_{aliphatic}$, 1668s (C=O), and 1625w (C=N). δ_H(600 MHz; $CDCl_3$) 5.36 (2 H, s, CH_2), 6.50, 6.51 (1 H, d, $CH_{aromatic}$), 6.78 (1 H, s, $CH_{aromatic}$), 6.91, 6.96 (1 H, m, $CH_{aromatic}$), 7.25–7.27 (6 H, t, $CH_{aromatic}$), 7.70 (6 H, s, $CH_{aromatic}$), 8.12 (2 H, s, $CH_{aromatic}$), 8.67 (2 H, s, $CH_{aromatic}$), 8.82 (1 H, s, N=CH), 11.70 (1 H, s, OH), and 13.27 (1 H, s, NH). δ_C(151 MHz; $CDCl_3$) 29.67, 29.98, 112.91, 113.50, 113.52, 116.70, 116.76, 117.51, 118.04, 118.13, 118.18, 118.27, 118.45, 122.14, 133.50, 137.06, 137.13, 137.20, 139.23, 150.28, 158.70, 161.91, 165.85, 165.88, and 167.60. δ^{19}_F(565 MHz; $CDCl_3$; $PhCF_3$) -98.80, -98.95, and -99.00. δ^{31}_P(243 MHz; $CDCl_3$; PPh_3) 20.74.

S1.3.3 Ligand {(*E*)-{4-hydroxy-3-{[2-(3-hydroxy-2-naphthoyl)hydrazono]methyl}benzyl}tris(4-fluorophenyl)phosphonium chloride (**[H$_3$L3]Cl**)

(0.037 g, 18.4 % after purification). mp 230 °C (decomposition). ν_{max}/cm^{-1} (FT-IR) 3031w (C–H)$_{aromatic}$, 2974w (C–H)$_{aliphatic}$, 1657s (C=O), and 1624m (C=N). δ_H(600 MHz; DMSO-d_6) 5.13, 5.15 (2 H, d, CH$_2$), 6.86–6.89 (2 H, t, CH$_{aromatic}$), 7.24 (1 H, s, CH$_{aromatic}$), 7.31–7.35 (2 H, t, CH$_{aromatic}$), 7.48–7.51 (1 H, t, CH$_{aromatic}$), 7.63–7.66 (6 H, m, CH$_{aromatic}$), 7.71–7.74 (1 H, m, CH$_{aromatic}$), 7.76–7.80 (6 H, m, CH$_{aromatic}$), 7.87–7.89 (1 H, t, CH$_{aromatic}$), 8.55 (1 H, s, CH$_{aromatic}$), 8.55 (1 H, s, N=CH), and 11.56 (1 H, s, OH). δ_C(151 MHz; DMSO-d_6) 27.81, 28.12, 110.51, 110.56, 110.58, 113.60, 113.62, 114.19, 114.21, 117.11, 117.58, 117.63, 117.73, 117.82, 117.88, 117.97, 119.70, 119.72, 120.04, 123.58, 123.60, 123.67, 125.78, 126.65, 128.18, 128.70, 130.06, 130.28, 130.95, 130.98, 133.27, 135.98, 137.28, 137.38, 137.45, 137.52, 146.60, 149.69, 154.87, 157.52, 164.34, 165.29, 165.31, 166.99, and 167.01. δ^{19}_F(565 MHz; DMSO-d_6; PhCF$_3$) -101,82. δ^{31}_P(243 MHz; DMSO-d_6; PPh$_3$) 21.05.

S1.4 Synthesis of the complexes **C1**–**C3**

The complexes were synthesized through one-pot in situ (template) reactions. In a 50 mL round bottom flask, 0.20 mmol of (3-formyl-4-hydroxybenzyl)tris(4-fluorophenyl)tris(4-fluorophenyl) chloride (**[AF]Cl**, 0.097 g) and 0.20 mmol of the respective hydrazide (**C1**: nicotinic, 0.027 g; **C2**: isonicotinic, 0.027 g, and **C3**: 3-hydroxy-2-naphthoic, 0.041 g) were solubilized in 10 mL (**C1**, **C2**) or 20 mL (**C3**) of methanol. The solution was maintained under constant magnetic stirring and heating in an oil bath at 70°C for 30 minutes. After this, 0.20 mmol of tris(acetylacetonate)vanadium(III) (V(acac)$_3$, 0.070 g) was added at 70°C. Then, 0.40 mmol of 1,8-diazabicyclo[5.4.0]undec-7-ene (DBU, 0.060 g, 60 µL) was added to the reaction. The reaction system was maintained under the same stirring and heating conditions at 70°C for more 2 hours (**Scheme S2**). The precipitation of **C3** was noted during the reaction.

The resulting brown mixture was filtered to remove any residual precipitate and the supernatant was added to small vials for air oxidation and slow evaporation of the solvent at room temperature. The obtained single crystals suitable for X-ray diffraction were separated, washed with hot methanol (10 mL) and dried at 50°C for 24 hours.

S1.4.1 Complex $[VO_2(L1)]\cdot H_2O$ (**C1**)

(Crystalline material: 0.050 g, 37.3 %). mp 204 °C (decomposition, from MeOH). (Found: C, 57.40; H, 3.60; N, 6.24. Calc. for $C_{32}H_{22}F_3N_3O_4PV\cdot H_2O$: C, 57.41; H, 3.61; N, 6.28 %). ν_{max}/cm^{-1} (FT-IR) 3542br $(O–H)_{water}$, 3038w $(C–H)_{aromatic}$, 2971w $(C–H)_{aliphatic}$, 1614m (C=N), 895s (V=O), and 828s (V=O). ν_{max}/cm^{-1} (FT-Raman) 1618w (C=N). δ_H(600 MHz; DMSO-d_6) 5.08, 5.10 (2 H, d, CH_2), 6.65, 6.67 (1 H, d, $CH_{aromatic}$), 6.84, 6.86 (1 H, d, $CH_{aromatic}$), 7.19 (1 H, s, $CH_{aromatic}$), 7.48–7.50 (1 H, m, $CH_{aromatic}$), 7.63–7.66 (6 H, m, $CH_{aromatic}$), 7.78–7.82 (6 H, m, $CH_{aromatic}$), 8.25, 8.27 (1 H, d, $CH_{aromatic}$), 8.66, 8.67 (1 H, d, $CH_{aromatic}$), 8.79 (1 H, s, N=CH), and 9.12 (1 H, s, $CH_{aromatic}$). δ^{19}_F(565 MHz; DMSO-d_6; $PhCF_3$) -101.95. δ^{31}_P(243 MHz; DMSO-d_6; PPh_3) 20.39. δ^{51}_V(158 MHz; DMSO-d_6; $VOCl_3/C_6D_6$) -537.19. *m/z* (ESI-MS) 652.05 ($[M+H]^+$, 100%). Calc. for $C_{32}H_{22}F_3N_3O_4PV$: 652.08.

S1.4.2 Complex $[VO_2(L2)]\cdot CH_3OH$ (**C2**)

(Crystalline material: 0.060 g, 43.9 %). mp 182 °C (decomposition, from MeOH). (Found: C, 56.49; H, 4.00; N, 5.98. Calc. for $C_{32}H_{22}F_3N_3O_4PV\cdot CH_3OH\cdot H_2O$: C, 56.50; H, 4.02; N, 5.99 %). ν_{max}/cm^{-1} (FT-IR) 3413br (O–H), 3052w $(C–H)_{aromatic}$, 2975w $(C–H)_{aliphatic}$, 1616m *v*(C=N), 922s (V=O), and 830s (V=O). ν_{max}/cm^{-1} (FT-Raman) 3073w $(C–H)_{aromatic}$ and 1615w (C=N). δ_H(600 MHz; DMSO-d_6) 5.08, 5.10 (2 H, d, CH_2), 6.66, 6.68 (1 H, d, $CH_{aromatic}$), 6.86, 6.87 (1 H, d, $CH_{aromatic}$), 7.19 (1 H, s, $CH_{aromatic}$), 7.63–7.66 (6 H, m, $CH_{aromatic}$), 7.77–7.82 (6 H, m, $CH_{aromatic}$), 7.84, 7.85 (2 H, d, $CH_{aromatic}$), 8.68, 8.69 (2 H, d, $CH_{aromatic}$), and 8.81 (1 H, s, N=CH). δ^{19}_F(565 MHz; DMSO-d_6; $PhCF_3$) -101.93. δ^{31}_P(243 MHz; DMSO-d_6; PPh_3) 20.41. δ^{51}_V(158 MHz; DMSO-d_6; $VOCl_3/C_6D_6$) -536.69. *m/z* (ESI-MS) 652.03 ($[M+H]^+$, 100%). Calc. for $C_{32}H_{22}F_3N_3O_4PV$: 652.08.

S1.4.3 Complex $[VO_2(HL3)]\cdot CH_3OH\cdot H_2O$ (**C3**)

(Crystalline material: 0.030 g, 19.6 %). mp 212 °C (decomposition, from MeOH). (Found: C, 59.50; H, 4.03; N, 3.63. Calc. for $C_{37}H_{25}F_3N_2O_5PV\cdot CH_3OH\cdot H_2O$: C, 59.54; H, 4.08; N, 3.65 %). ν_{max}/cm^{-1} (FT-IR) 3505br $(O–H)_{water}$, 3060w $(C–H)_{aromatic}$, 2979w $(C–H)_{aliphatic}$, 1613m (C=N), 904s (V=O), and 831s (V=O). ν_{max}/cm^{-1} (FT-Raman) 3067w $(C–H)_{aromatic}$ and 1618m (C=N). δ_H(600 MHz; DMSO-d_6) 5.10, 5.12 (2 H, d, CH_2), 6.69, 6.70 (1 H, d, $CH_{aromatic}$), 6.87, 6.88 (1 H, d, $CH_{aromatic}$), 7.23 (1 H, s, $CH_{aromatic}$), 7.30–7.33 (2 H, m, $CH_{aromatic}$), 7.47–7.49 (1 H, t, $CH_{aromatic}$), 7.63–7.66 (6 H, m, $CH_{aromatic}$), 7.74, 7.75 (1 H, d, $CH_{aromatic}$), 7.78–7.82 (6 H, m, $CH_{aromatic}$), 7.95, 7.96 (1 H, d, $CH_{aromatic}$), 8.49 (1 H, s, $CH_{aromatic}$), 8.96 (1 H, s, N=CH), and 12.00 (1 H, s, $OH_{naphthoic}$). δ^{19}_F(565 MHz; DMSO-d_6; $PhCF_3$) -101.89. δ^{31}_P(243 MHz; DMSO-d_6; PPh_3) 20.41. δ^{51}_V(158 MHz; DMSO-d_6; $VOCl_3/C_6D_6$) -538.71. *m/z* (ESI-MS) 717.08 ($[M+H]^+$, 100%). Calc. for $C_{37}H_{25}F_3N_2O_5PV$: 717.09.

Tables

Table S1 Crystal data and structure refinement for **C1**–**C3**

	C1	**C2**	**C3**
Empirical formula	$C_{32}H_{24}F_3N_3O_5PV$	$C_{66}H_{52}F_6N_6O_{10}P_2V_2$	$C_{38}H_{31}F_3N_2O_7PV$
Formula weight	669.45	1366.96	766.56
Temperature (K)	100(2)	100(2)	100(2)
Wavelength (Å)	0.71073 (Mo–Kα)	0.71073 (Mo–Kα)	0.71073 (Mo–Kα)
Crystal system, space group	Triclinic, $P\bar{1}$	Triclinic, $P\bar{1}$	Monoclinic, $P2_1/c$
$a \times b \times c$ (Å)	10.118(8) × 11.742(9) × 14.272(12)	14.696(4) × 14.852(4) × 16.796(4)	11.288(4) × 20.111(7) × 15.857(5)
$\alpha \times \beta \times \gamma$ (º)	69.73(3) × 72.48(3) × 73.77(3)	111.604(7) × 91.134(8) × 111.054(8)	90 × 105.698(10) × 90
Volume ($Å^3$)	1487(2)	3131.7(14)	3466(2)
Z, C. density (mg m^{-3})	2, 1.495	2, 1.450	4, 1.469
Absorp. Coeffic. (mm^{-1})	0.453	0.432	0.403
F (000)	684	1400	1576
Crystal size (mm)	0.341 × 0.212 × 0.118	0.22 × 0.19 × 0.12	0.38 × 0.19 × 0.18
Theta range for data collection (°)	2.08 to 27.99	1.92 to 26.91	2.03 to 24.84
Limiting indices	-13 ≤ h ≤ 13, -15 ≤ k ≤ 15, -18 ≤ l ≤ 18	-18 ≤ h ≤ 16, -18 ≤ k ≤ 18, -21 ≤ l ≤ 21	-10 ≤ h ≤ 13, -19 ≤ k ≤ 19, -15 ≤ l ≤ 15
Reflections collected/unique	44357/7172	43401/13490	25487/3144
Completeness to theta	99.8 %	99.5 %	99.5 %
Absorption correction	Semi-empirical from equivalents	Semi-empirical from equivalents	Semi-empirical from equivalents
Max. and min. trans.	0.7456 and 0.7039	0.9700 and 0.9210	0.9211 and 0.85621
Refinement method	Full-matrix least-squares on F^2	Full-matrix least-squares on F^2	Full-matrix least-squares on F^2
Data/restraints/ parameters	7172/0/406	13490/0/833	3144/1/471
Goodness-of-fit on F^2	0.991	1.008	1.250

Indice R_{int}	0.0446	0.1111	0.0558
Final R indices R_1 and $wR_2[I>2\sigma(I)]$	R1 = 0.0474, wR2 = 0.1295	R1 = 0.0951, wR2 = 0.1650	R1 = 0.0621, wR2 = 0.1644
R indices (all data)	R1 = 0.0623, wR2 = 0.1394	R1 = 0.1123, wR2 = 0.1034	R1 = 0.0742, wR2 = 0.1822
Largest diff. peak and hole (e.Å^{-3})	0.340 and -0.530	0.506 and -0.421	0.567 and -0.400

Table S2 Values of selected bond lengths (Å) of **C1**–**C3** and dioxidovanadium(V) complexes from literature

	Bond length values (Å)					
Bond	**C1**	**C2***	**C3**	**Complex from literature[5]*** (nicotinic hydrazide)	**Complex from literature[5]** (isonicotinic hydrazide)	**Complex from literature[6]** (3-hydroxy-2-naphthoic hydrazide)
V^V–N(imine)	2.155(2)	2.138(5)/ 2.147(4)	2.145(5)	2.133(4)/ 2.165(4)	2.139(5)	2.1505(12)
V^V–O (phenolate)	1.914(2)	1.907(4)/ 1.902(4)	1.898(5)	1.891(3)/ 1.915(3)	1.914(3)	1.9017(12)
V^V–O (enolate)	1.976(2)	1.981(4)/ 1.982(4)	1.973(5)	1.967(3)/ 1.980(3)	1.978(4)	1.9822(11)
V^V=O (oxido)	1.621(2), 1.644(2)	1.609(4), 1.612(4)/ 1.602(4), 1.622(4)	1.588(6), 1.595(6)	1.599(4), 1.661(3)/ 1.601(4), 1.660(3)	1.607(4), 1.634(4)	1.6106(14), 1.6358(13)
N(imine)–N(amide)	1.396(3)	1.413(6)/ 1.396(6)	1.395(8)	1.398(5)/ 1.404(5)	1.406(5)	1.3921(17)
C–N(amide)	1.312(3)	1.294(7)/ 1.292(7)	1.295(9)	1.306(6)/ 1.304(6)	1.288(6)	1.3105(19)
C–O(enolate)	1.304(3)	1.288(6)/ 1.304(7)	1.296(8)	1.313(6)/ 1.288(6)	1.304(6)	1.3008(18)

* = Two independent units of the complex in the asymmetric unit.

Table S3 Values of selected bond angles (°) of **C1**–**C3** and dioxidovanadium(V) complexes from literature

	Bond angle values (°)					
Angle	**C1**	**C2***	**C3**	**Complex from literature*** [5] (nicotinic hydrazide)	**Complex from literature** [6] (isonicotinic hydrazide)	**Complex from literature** [6] (3-hydroxy-2-naphthoic hydrazide)
N(imine)–V^V–O (phenolate)	81.86(9)	82.02(17)/ 82.42(16)	82.3(2)	81.75(15)/ 82.30(14)	82.35(15)	81.79(5)
N(imine)–V^V–O (enolate)	74.0(10)	73.59(17)/ 73.57(16)	73.1(2)	74.20(14)/ 73.73(13)	73.68(15)	73.53(4)
N(imine)–V^V=O(oxido)	104.64(10), 145.77(11)	124.5(2), 125.6(2)/ 114.3(2), 136.2(2)	119.5(4), 129.8(3)	103.52(17), 149.08(18)/ 97.27(18), 156.79(17)	113.49(18), 137.27(18)	112.22(7), 136.99(7)
O (phenolate)–V^V–O (enolate)	147.59(8)	155.46(17)/ 153.50(18)	154.9(2)	146.58(16)/ 150.05(14)	153.37(17)	151.65(5)
O(oxido)= V^V–O (phenolate)	95.27(12), 105.63(10)	98.0(2), 100.6(2)/ 96.0(2), 101.4(2)	97.5(3), 98.8(3)	95.27(16), 105.19(18)/ 98.09(16), 101.72(18)	97.09(16), 101.82(19)	96.32(6), 100.97(7)
O(oxido)= V^V–O (enolate)	92.79(11), 101.26(10)	94.1(2), 95.48(19)/ 93.7(2), 98.6(2)	94.7(3), 97.4(3)	93.74(15), 102.78(16)/ 97.10(15), 98.93(16)	92.86(17), 98.31(19)	92.43(5), 101.14(6)
O(oxido)= V^V =O(oxido)	108.93(13)	109.1(2)/ 108.9(2)	110.2(5)	106.93(19)/ 105.30(19)	108.5(2)	110.31(9)
C–N(amide)–N(imine)	108.05(18)	108.3(5)/ 109.0(5)	108.3(6)	108.2(4)/ 108.1(4)	107.9(4)	109.2(1)

* = Two independent units of the complex in the asymmetric unit.

Table S4 The β and α angles (°), calculated τ values (dimensionless), and coordination geometries of **C1**–**C3** and dioxidovanadium(V) complexes from literature

Complex	β (°)[a]	α (°)[b]	τ[c]	Coordination geometry
C1	147.59(8)	145.77(11)	0.03	Slightly distorted square based pyramid
C2*	155.46(17)/ 153.50(18)	125.6(2)/ 136.2(2)	0.50/ 0.29	Distorted between square based pyramid and trigonal bipyramid/ distorted square based pyramid
C3	154.9(2)	129.8(3)	0.42	Distorted between square based pyramid and trigonal bipyramid
Complex from literature*[5] (nicotinic hydrazide)	149.08(18)/ 156.79(17)	146.58(16)/ 150.05(14)	0.04/ 0.11	Slightly distorted square based pyramid/slightly distorted square based pyramid
Complex from literature[6] (isonicotinic hydrazide)	153.37(17)	137.27(18)	0.26	Distorted square based pyramid
Complex from literature[6] (3-hydroxy-2-naphthoic hydrazide)	151.65(5)	136.99(7)	0.24	Distorted square based pyramid

a = Highest bond angle value; b = Second highest bond angle value; c = Structural index parameter τ (dimensionless) calculated[7] as $\tau = (\beta - \alpha)/60$; * = Two independent units of the complex in the asymmetric unit.

Table S5 Molecular docking results for the interaction between deoxyribonucleic acid and **C1**–**C3** in the minor groove

System	Nucleobase	Interaction	Distance (Å)
DNA:**C1**	DA-05	Van der Waals	4.00
	DA-06	Van der Waals	3.50
	DT-07	Van der Waals	3.20
	DA-18	Van der Waals	3.90
	DT-19	Van der Waals	3.10
	DT-20	Van der Waals	3.90
DNA:**C2**	DG-04	Van der Waals	3.30
	DA-05	Van der Waals	4.00
	DA-06	Van der Waals	4.10
	DT-20	Van der Waals	4.00
	DG-22	Van der Waals	4.00
DNA:**C3**	DA-05	Van der Waals	4.00
	DA-06	Van der Waals	3.30
	DT-07	Van der Waals	2.30
	DA-18	Van der Waals	3.00
	DT-19	Van der Waals	2.30
	DT-20	Van der Waals	3.30

DA, adenine; DT, thymidine; DG, guanine.

Table S6 Molecular docking results for the interaction between bovine serum albumin and **C1**–**C3** in the site III

System	Amino acid residue	Interaction	Distance (Å)
BSA:**C1**	Leu-116	Hydrophobic	3.57
	Pro-118	Hydrophobic	3.91
	Leu-123	Hydrophobic	3.35
	Glu-126	Hydrophobic	3.43
	Phe-134	Hydrophobic	3.27
	Lys-137	Hydrophobic	3.40
	Lys-137	π-cation	3.55
	Tyr-138	Hydrogen bond	2.09
	Tyr-138	Hydrophobic	3.56

	Glu-141	Hydrophobic	3.35
	Tyr-161	Hydrogen bond	2.09
	Tyr-161	π-stacking	5.29
	Ile-182	Hydrophobic	3.50
	Met-185	Hydrophobic	3.91
	Arg-186	Hydrogen bond	2.96
	Arg-186	Hydrophobic	3.67
BSA:**C2**	Pro-118	Hydrophobic	3.74
	Leu-123	Hydrophobic	3.44
	Glu-126	Hydrophobic	3.70
	Phe-134	Hydrophobic	3.31
	Lys-137	π-cation	3.53
	Lys-137	Hydrophobic	3.46
	Tyr-138	Hydrogen bond	2.63
	Tyr-138	Hydrophobic	3.21
	Glu-141	Hydrophobic	3.13
	Ile-142	Hydrophobic	3.81
	Tyr-161	Hydrogen bond	2.19
	Tyr-161	Hydrophobic	3.53
	Ile-182	Hydrophobic	3.41
BSA:**C3**	Leu-116	Hydrophobic	3.40
	Pro-118	Hydrophobic	3.39
	Leu-123	Hydrophobic	2.71
	Phe-134	Hydrophobic	3.55
	Lys-137	Hydrophobic	3.26
	Lys-137	π-cation	3.33
	Tyr-138	Hydrophobic	3.48
	Tyr-161	Hydrogen bond	1.67
	Glu-183	Hydrogen bond	3.30
	Arg-186	π-cation	3.58

Leu, leucine; Pro, proline; Val, valine; Arg, arginine; Tyr, tirosine; Glu, glutamic acid; Ile, Isoleucine; Phe, phenylalanine; Lys, lysine; Met, methionine.

Table S7 Molecular docking results for the interaction between human serum albumin and **C1**–**C3** in the site III

System	Amino acid residue	Interaction	Distance (Å)
HSA:**C1**	Leu-115	Hydrophobic	3.37
	Arg-117	Hydrophobic	3.36
	Arg-117	Hydrogen bond	3.13
	Phe-134	Hydrophobic	3.73
	Lys-137	Hydrophobic	3.35
	Tyr-138	Hydrophobic	3.51
	Glu-141	Hydrophobic	3.45
	Ile-142	Hydrophobic	3.58
	Tyr-161	Hydrogen bond	2.70
	Leu-182	Hydrophobic	3.75
	Arg-186	Hydrophobic	3.73
HSA:**C2**	Leu-115	Hydrophobic	3.38
	Arg-117	Hydrophobic	3.40
	Arg-117	Hydrogen bond	2.99
	Phe-134	Hydrophobic	3.47
	Lys-137	Hydrophobic	3.29
	Tyr-138	Hydrophobic	3.35
	Glu-141	Hydrophobic	3.36
	Leu-182	Hydrophobic	3.95
	Arg-186	Hydrogen bond	3.22
HSA:**C3**	Leu-115	Hydrophobic	3.31
	Arg-117	Hydrophobic	3.58
	Arg-117	Hydrogen bond	3.06
	Phe-134	Hydrophobic	3.74
	Lys-137	Hydrophobic	3.29
	Tyr-138	Hydrophobic	3.53
	Tyr-138	Hydrogen bond	1.82
	Glu-141	Hydrophobic	3.81
	Ile-142	Hydrophobic	3.56
	Tyr-161	π stacking	4.98
	Leu-182	Hydrophobic	3.32

Leu-185	Hydrogen bond	3.15
Arg-186	Hydrophobic	3.75
Lys-190	Hydrophobic	3.33

Leu, leucine; Val, valine; Arg, arginine; Tyr, tirosine; Glu, glutamic acid; Ile, Isoleucine; Phe, phenylalanine; Lys, lysine; Ala, alanine; Asn, asparagine; Thr, threonine.

Figures

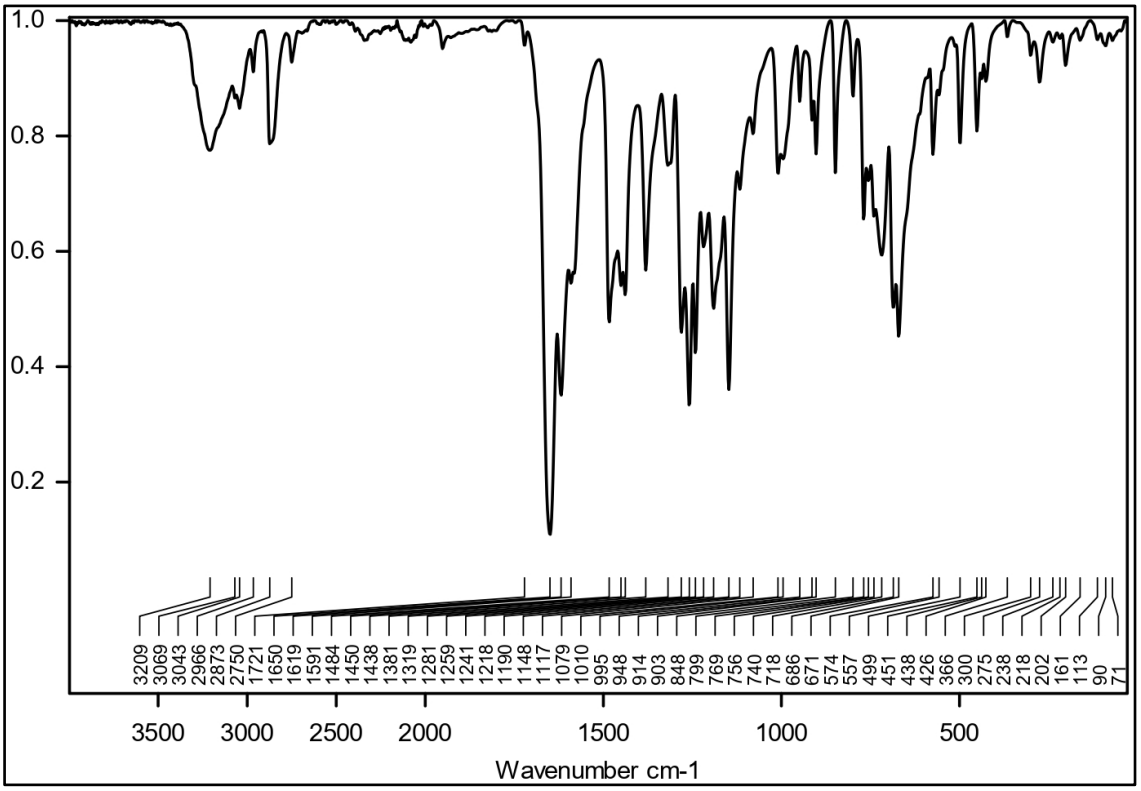

Fig. S1 FT-IR spectrum of 5-(chloromethyl)-2-hydroxybenzaldehyde (ATR).

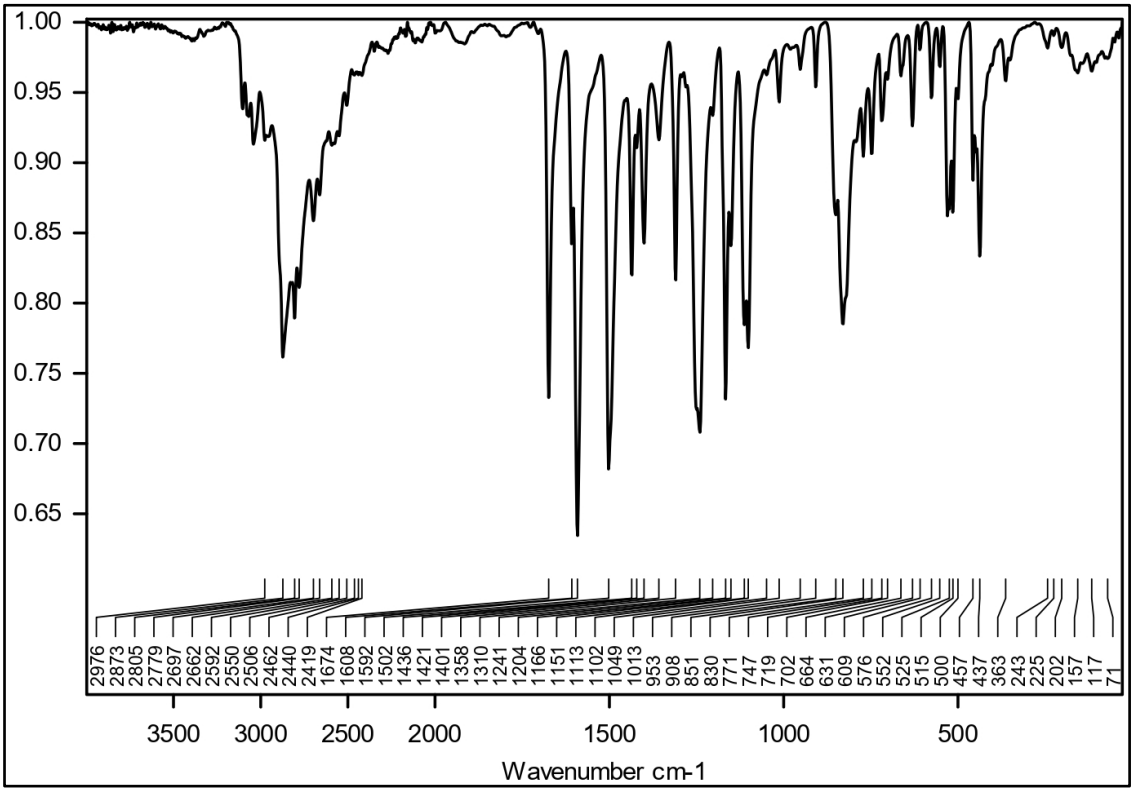

Fig. S2 FT-IR spectrum of **[AF]Cl** (ATR).

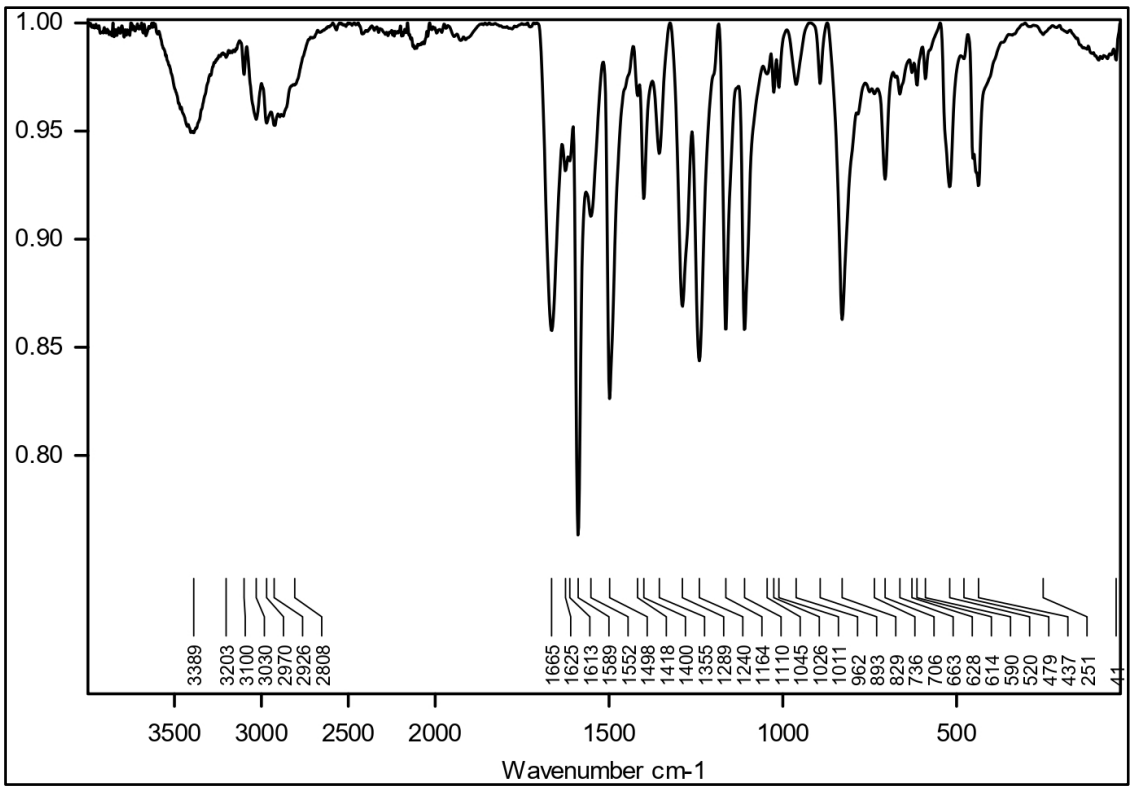

Fig. S3 FT-IR spectrum of **[H_2L1]Cl** (ATR).

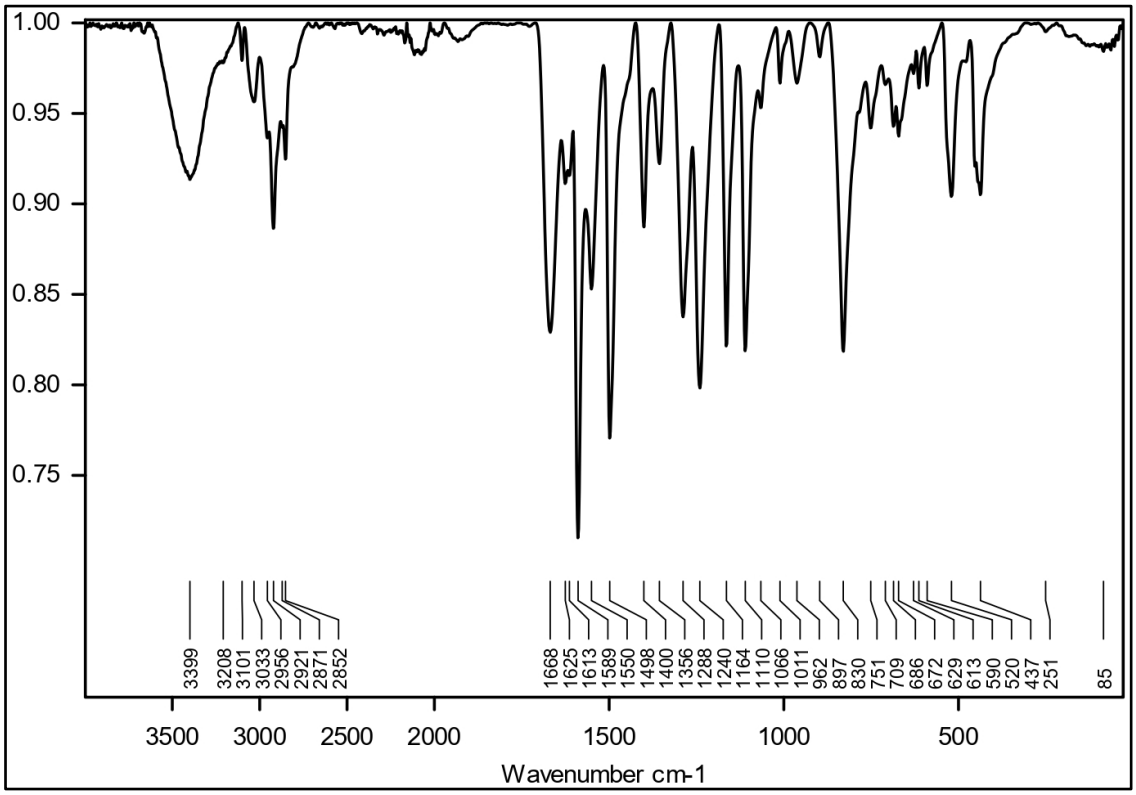

Fig. S4 FT-IR spectrum of **[H_2L2]Cl** (ATR).

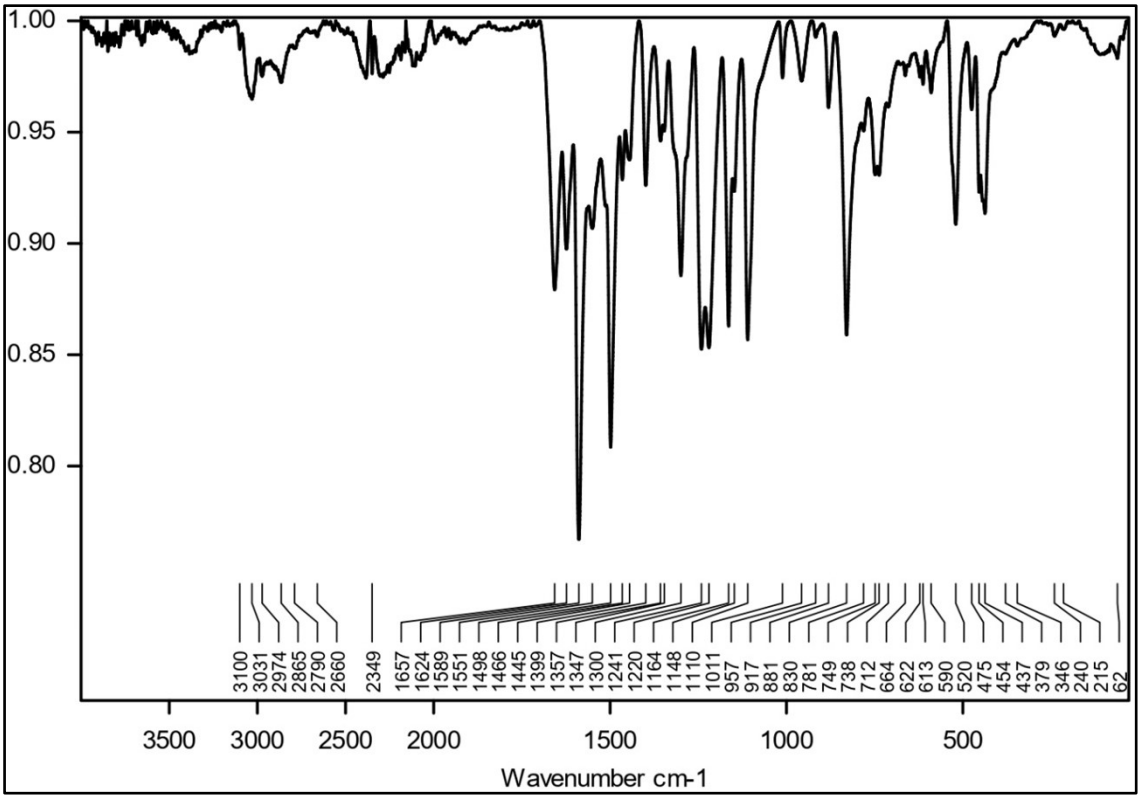

Fig. S5 FT-IR spectrum of **[H_3L3]Cl** (ATR).

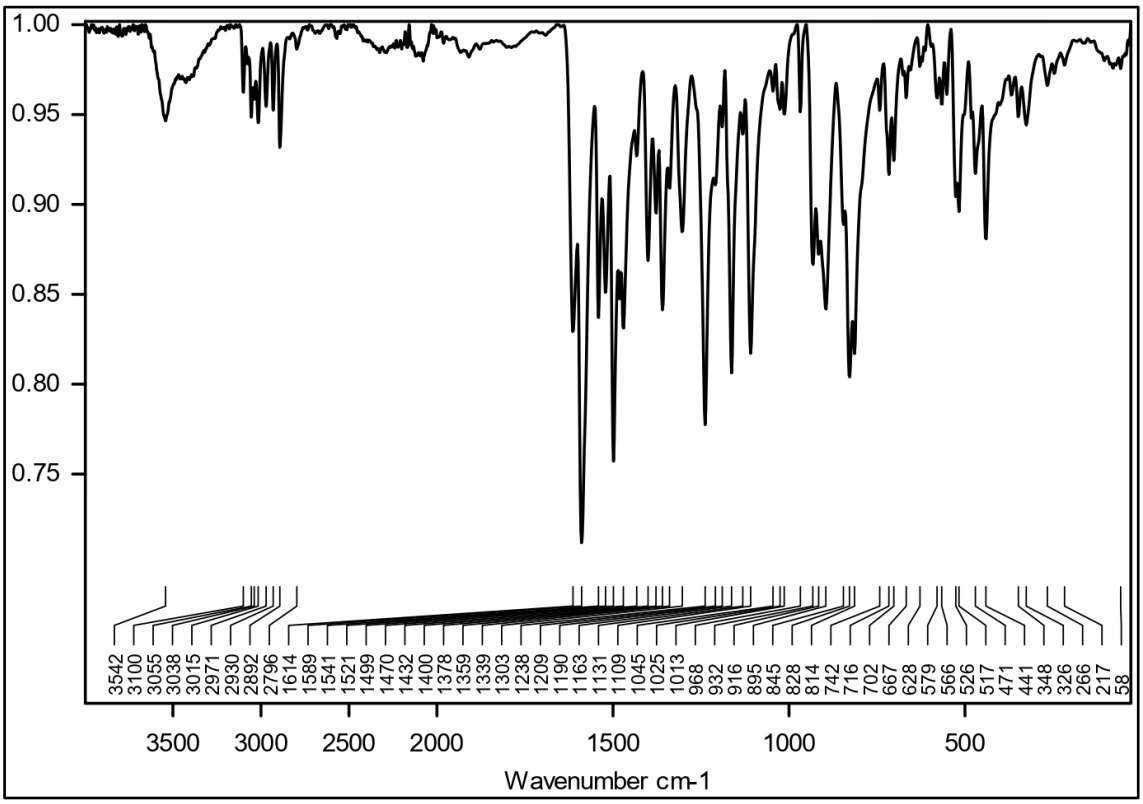

Fig. S6 FT-IR spectrum of $[VO_2L1]\cdot H_2O$ (**C1**) (ATR).

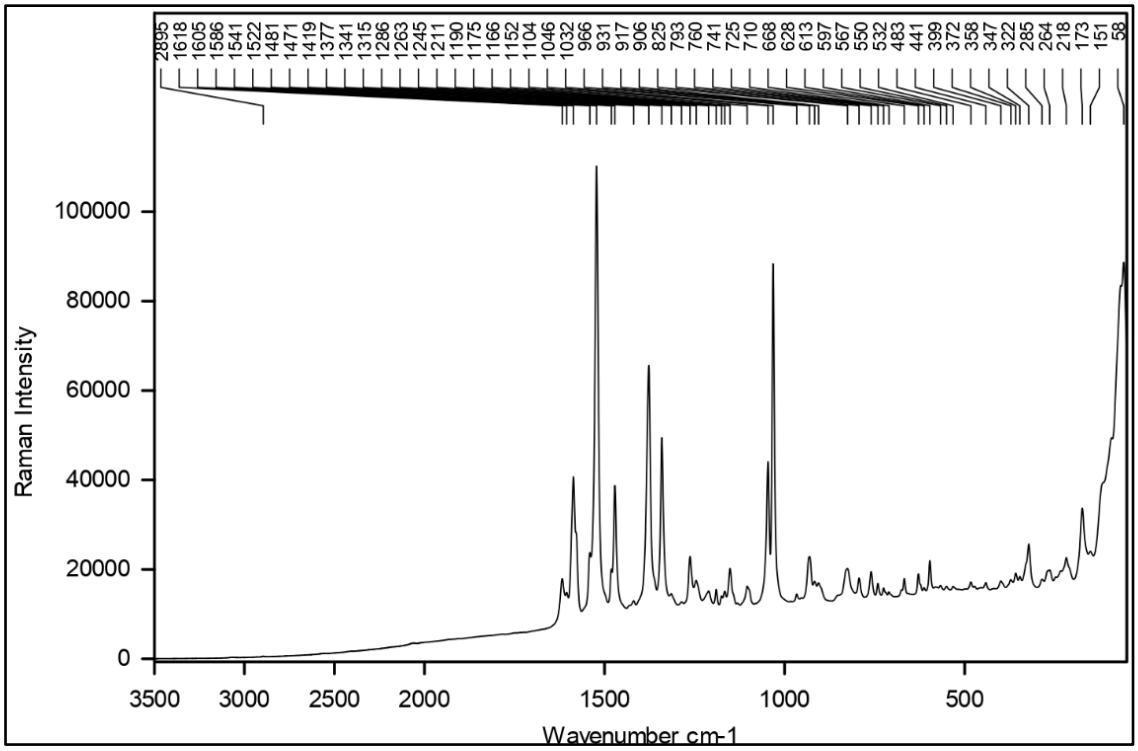

Fig. S7 FT-Raman spectrum of $[VO_2L1]\cdot H_2O$ (**C1**) (785 nm, 25 mW, 6 coadditions of 10 s).

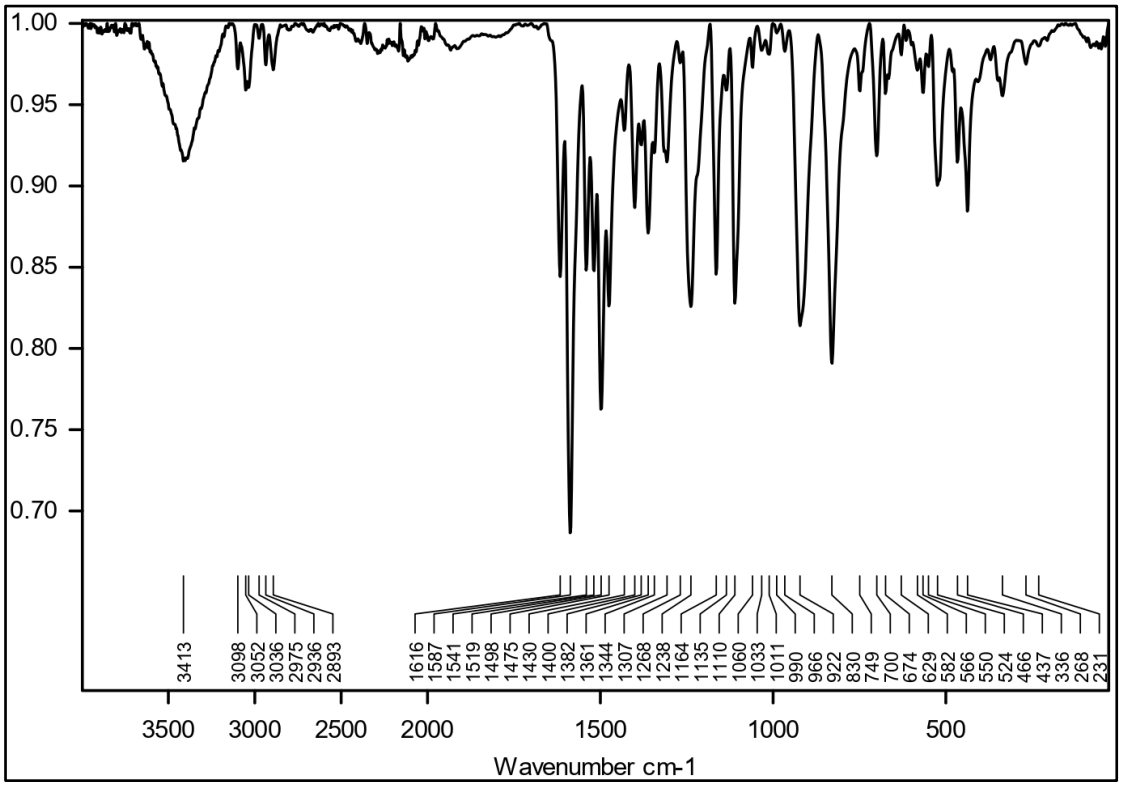

Fig. S8 FT-IR spectrum of $[VO_2L2]\cdot CH_3OH$ (**C2**) (ATR).

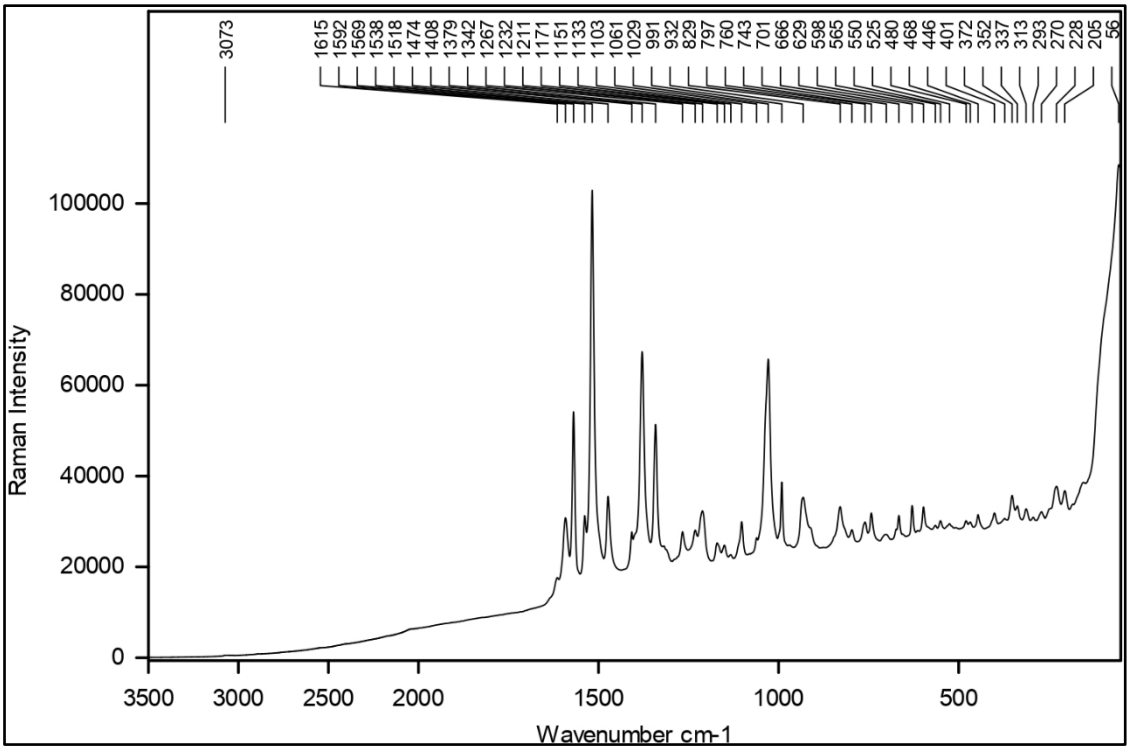

Fig. S9 FT-Raman spectrum of $[VO_2L2]\cdot CH_3OH$ (**C2**) (785 nm, 25 mW, 6 coadditions of 10 s).

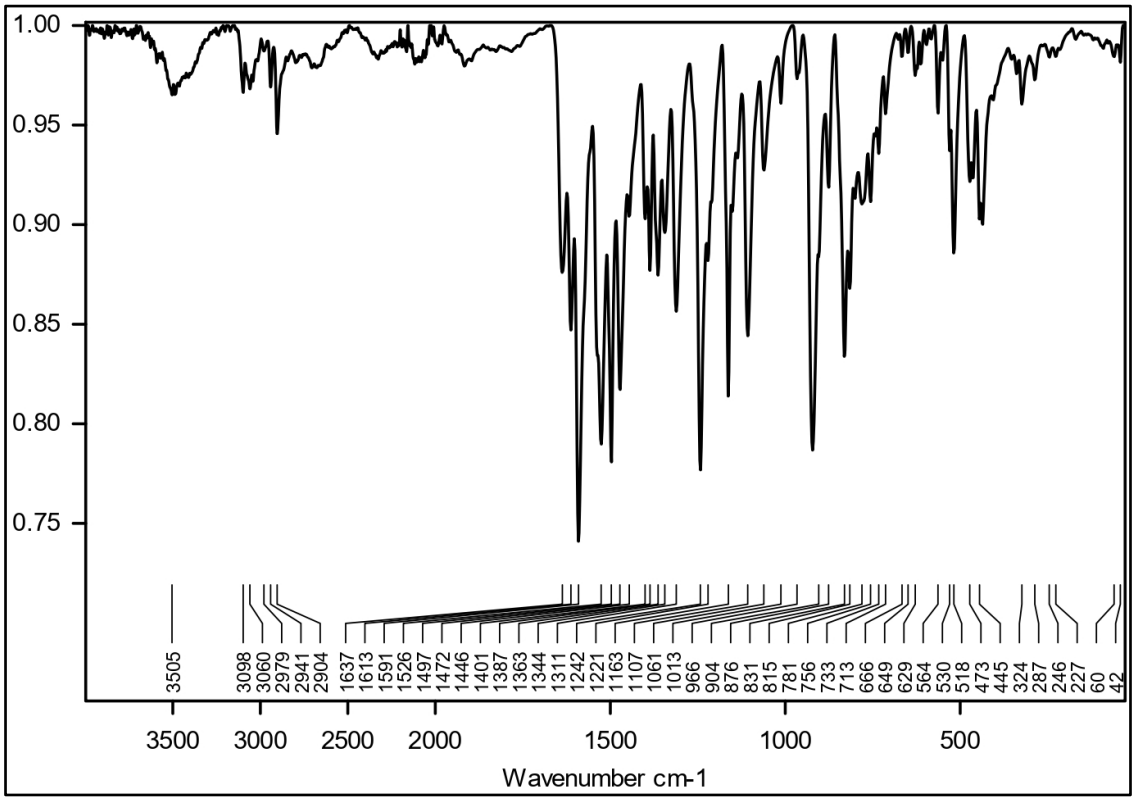

Fig. S10 FT-IR spectrum of $[VO_2HL3]\cdot CH_3OH\cdot H_2O$ (**C3**) (ATR).

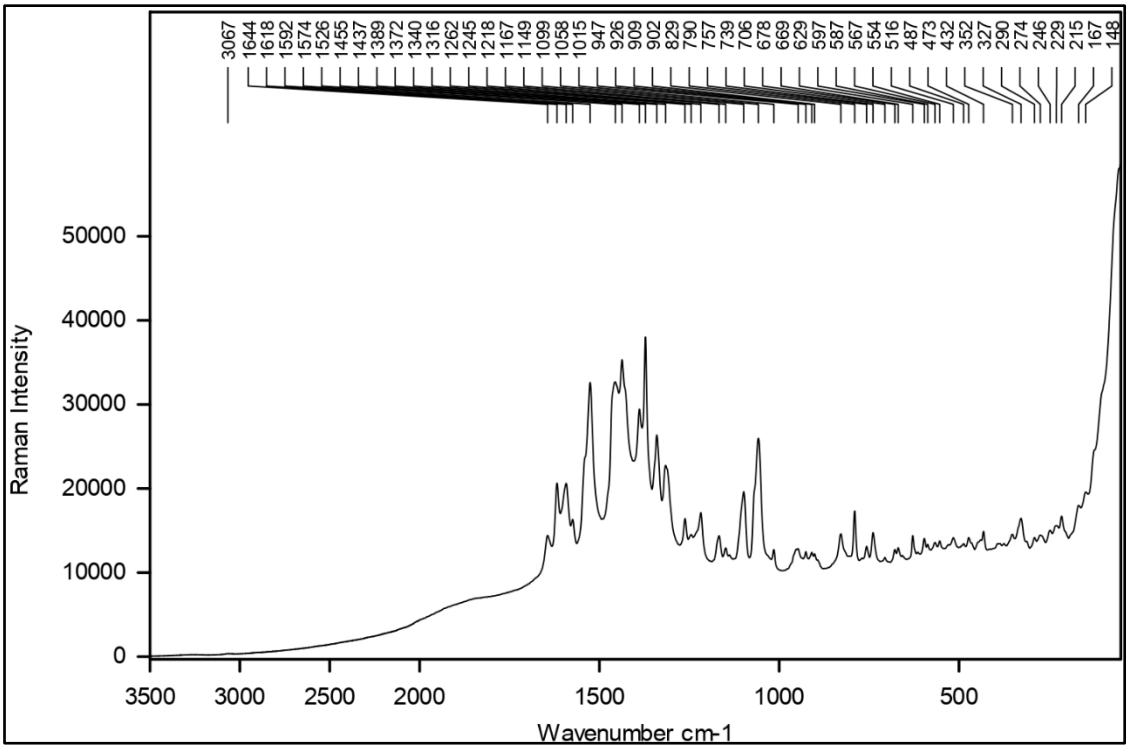

Fig. S11 FT-Raman spectrum of $[VO_2HL3]\cdot CH_3OH\cdot H_2O$ (**C3**) (785 nm, 25 mW, 6 coadditions of 10 s).

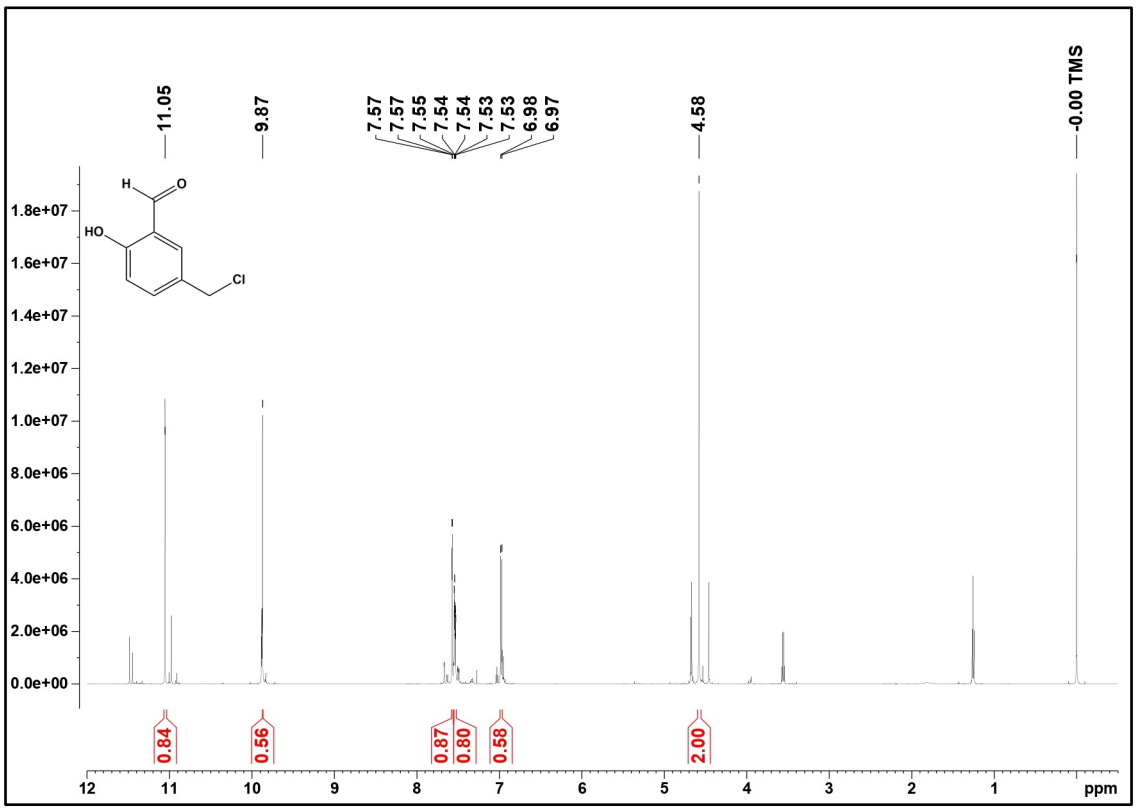

Fig. S12 ^{1}H-NMR spectra of 5-(chloromethyl)-2-hydroxybenzaldehyde (600 MHz, $CDCl_3$).

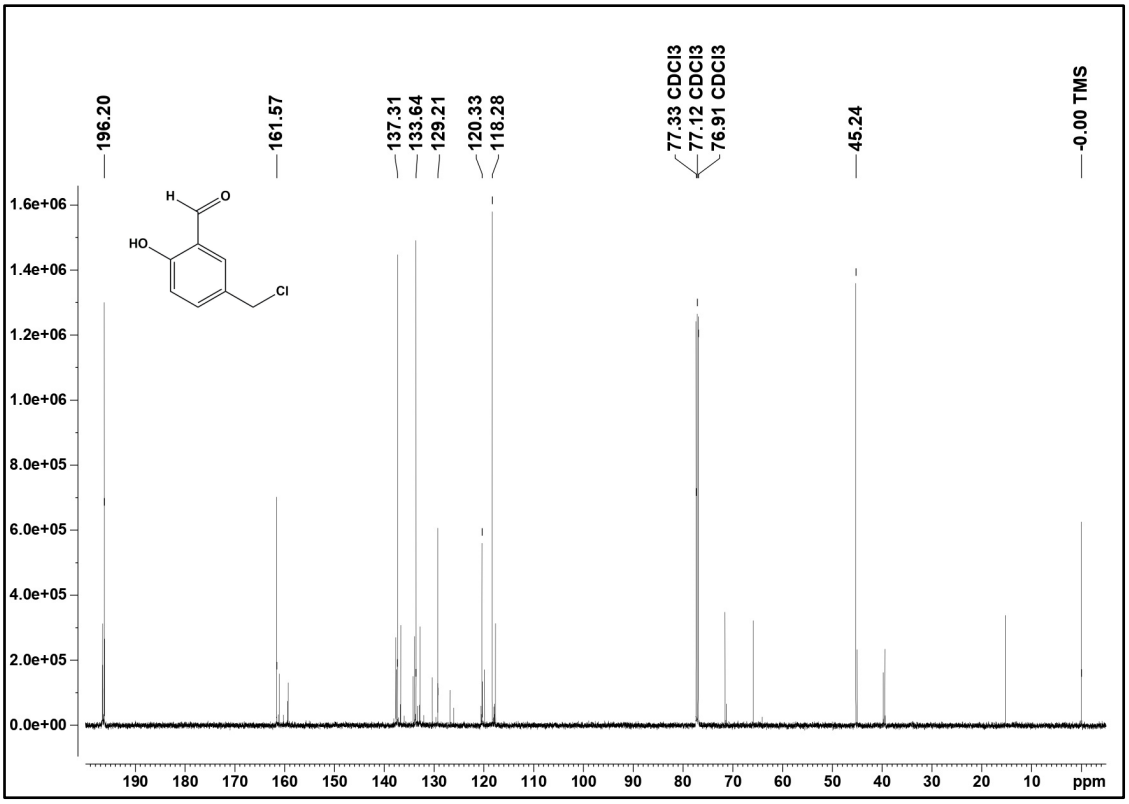

Fig. S13 ^{13}C-NMR spectra of 5-(chloromethyl)-2-hydroxybenzaldehyde (151 MHz, $CDCl_3$).

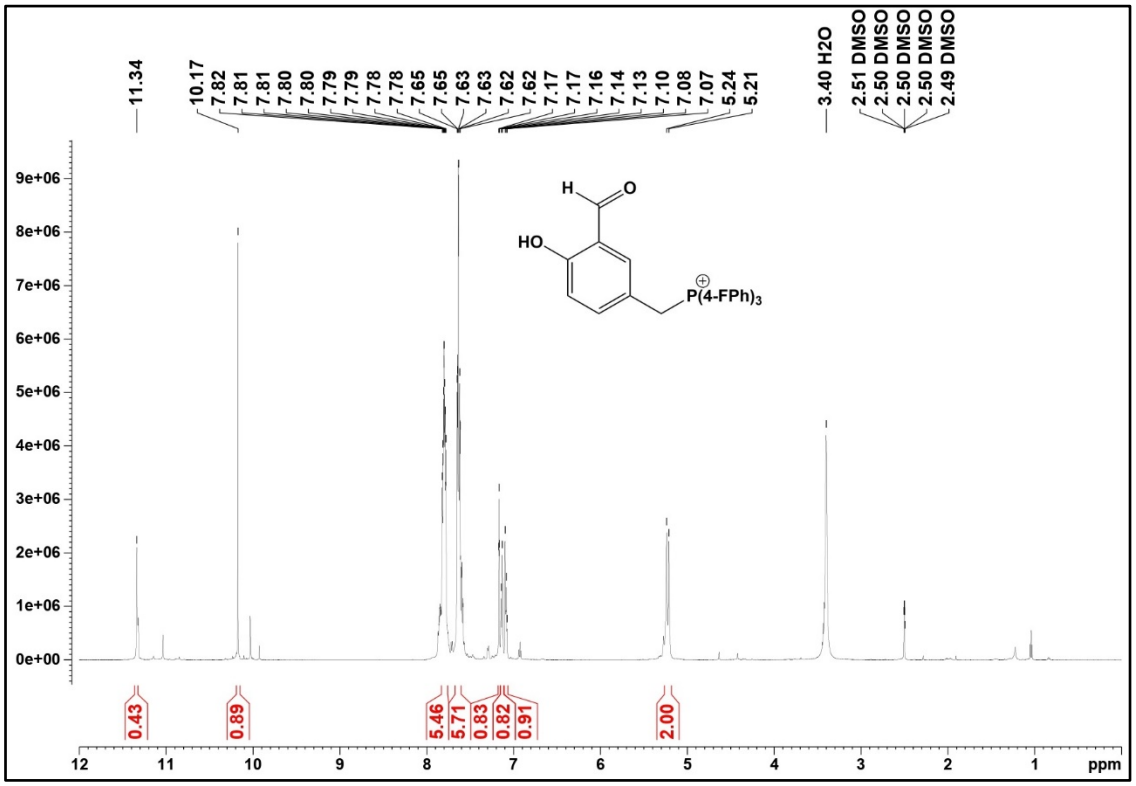

Fig. S14 ^{1}H-NMR spectra of **[AF]Cl** (600 MHz, DMSO-d_6).

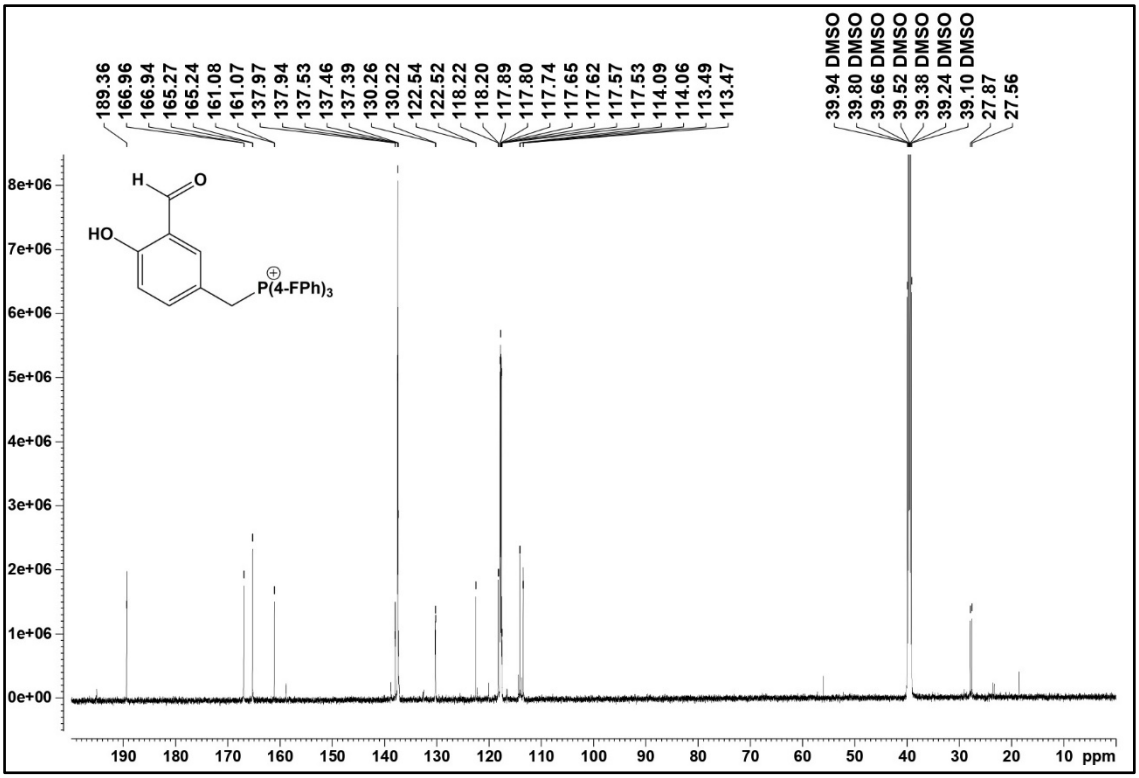

Fig. S15 ^{13}C-NMR spectra of **[AF]Cl** (151 MHz, DMSO-d_6).

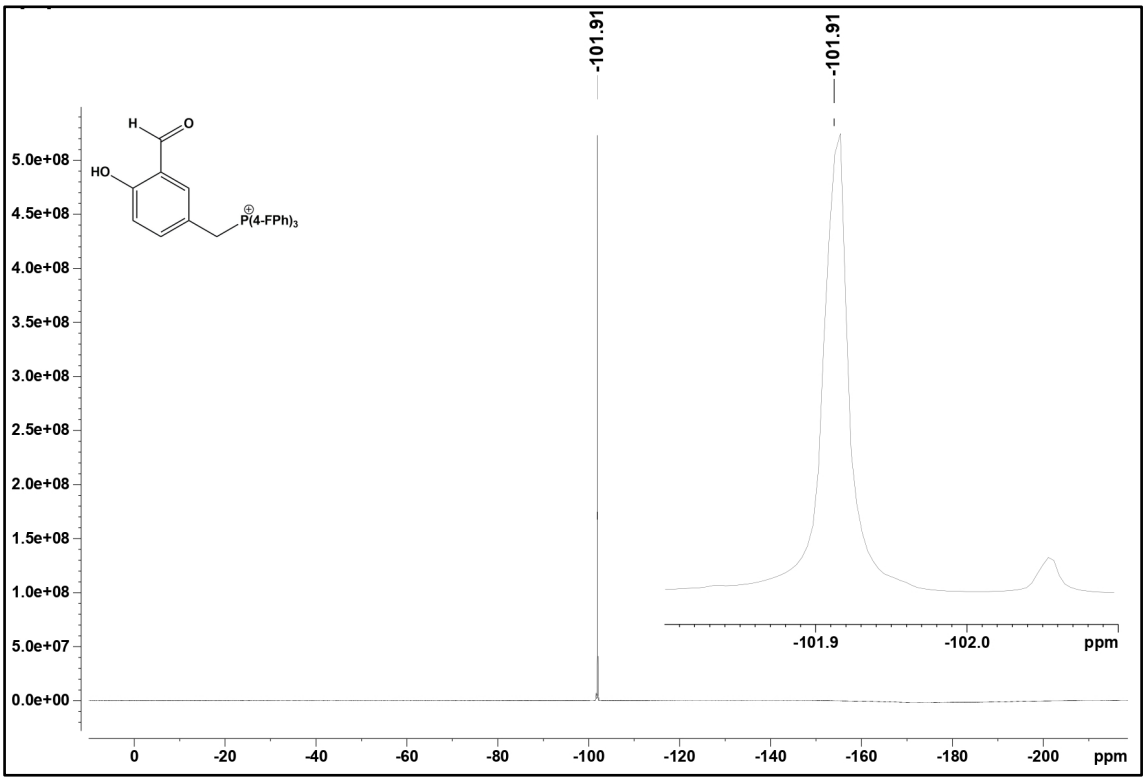

Fig. S16 ^{19}F-NMR spectra of **[AF]Cl** (565 MHz, DMSO-d_6).

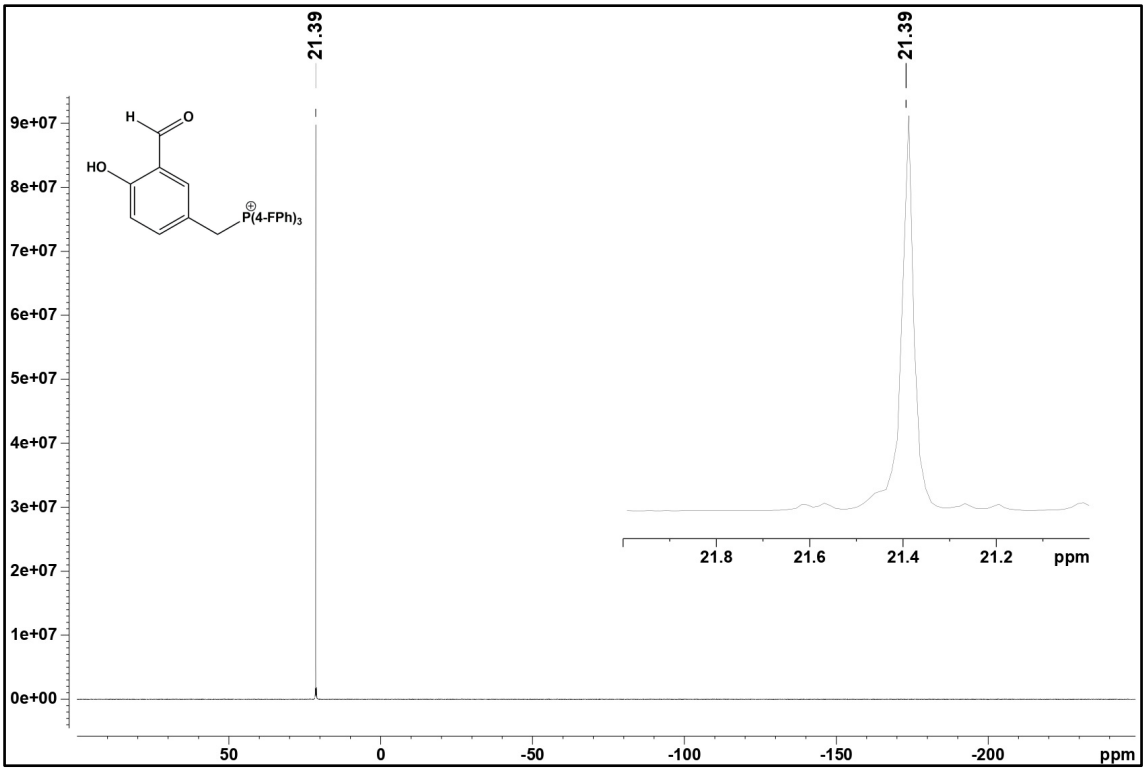

Fig. S17 ^{31}P-NMR spectra of **[AF]Cl** (243 MHz, DMSO-d_6).

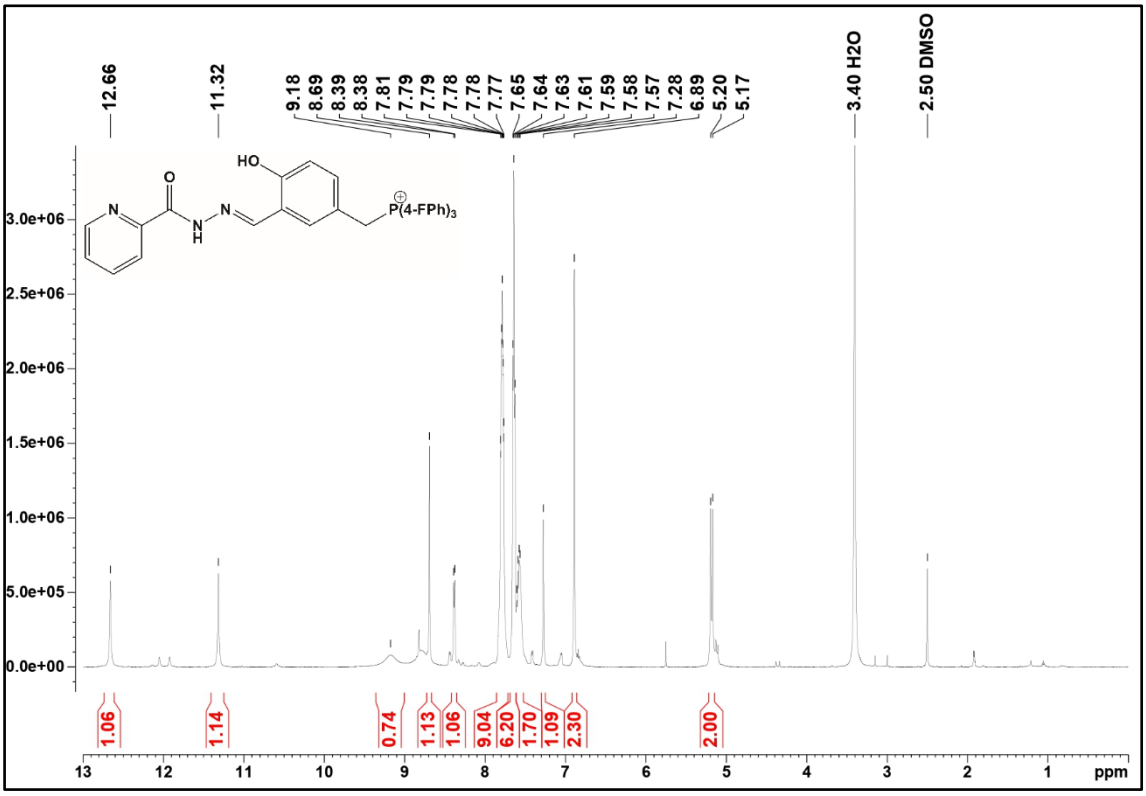

Fig. S18 ^{1}H-NMR spectra of **[H_2L1]Cl** (600 MHz, DMSO-d_6).

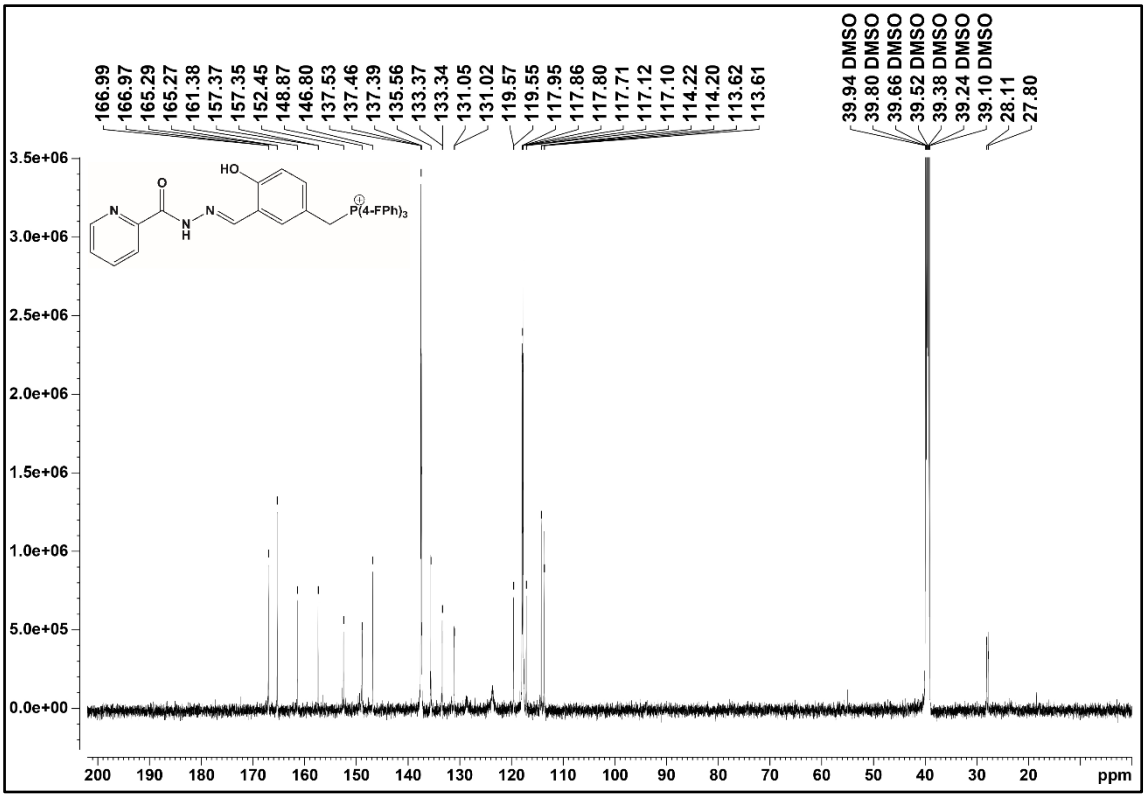

Fig. S19 ^{13}C-NMR spectra of **[H_2L1]Cl** (151 MHz, DMSO-d_6).

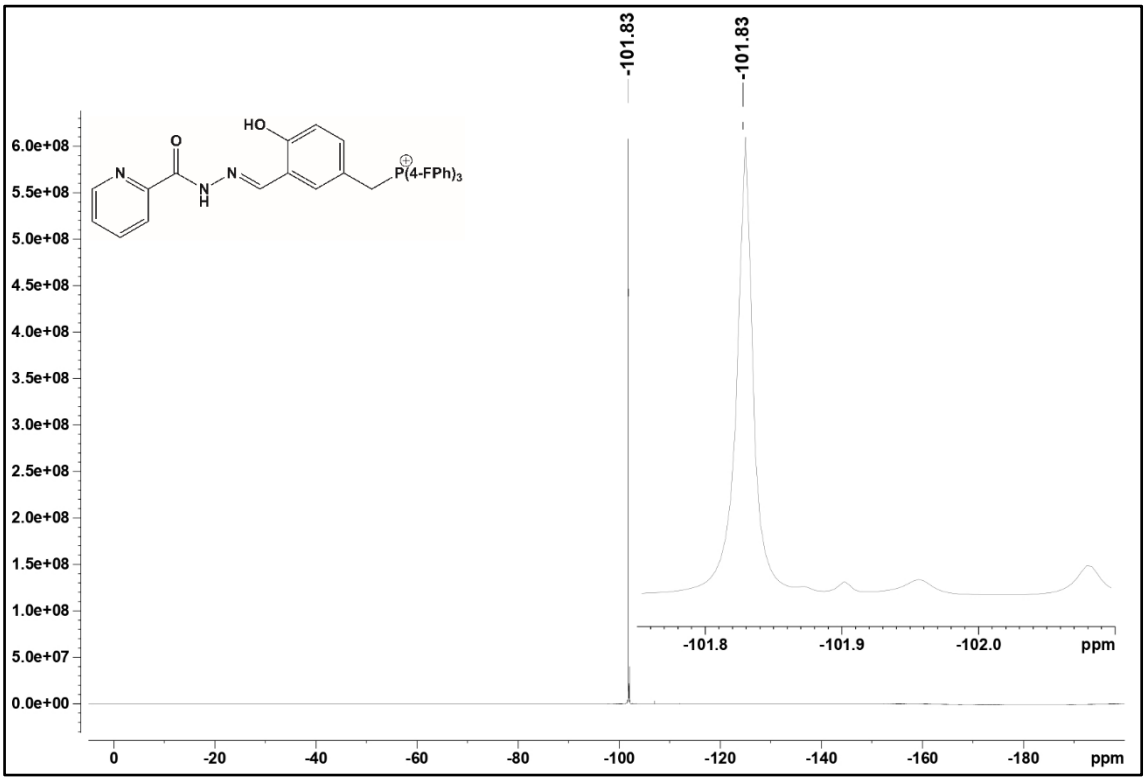

Fig. S20 ^{19}F-NMR spectra of **[H_2L1]Cl** (565 MHz, DMSO-d_6).

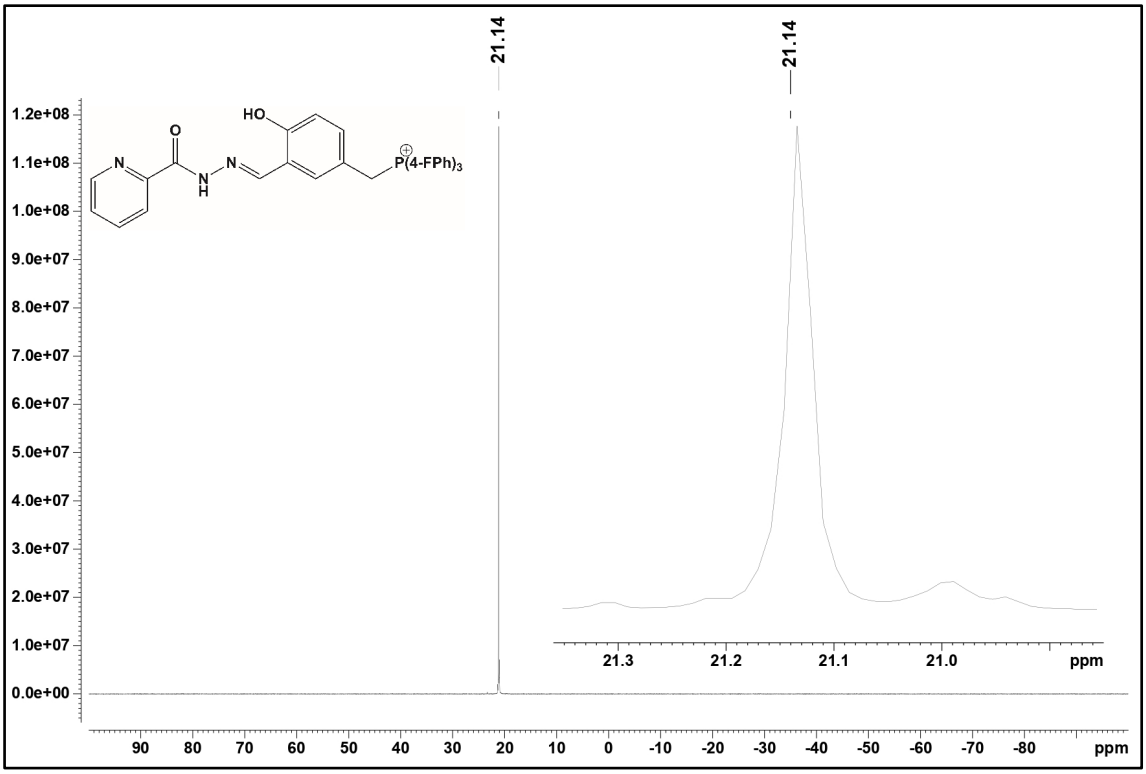

Fig. S21 ^{31}P-NMR spectra of **[H_2L1]Cl** (243 MHz, DMSO-d_6).

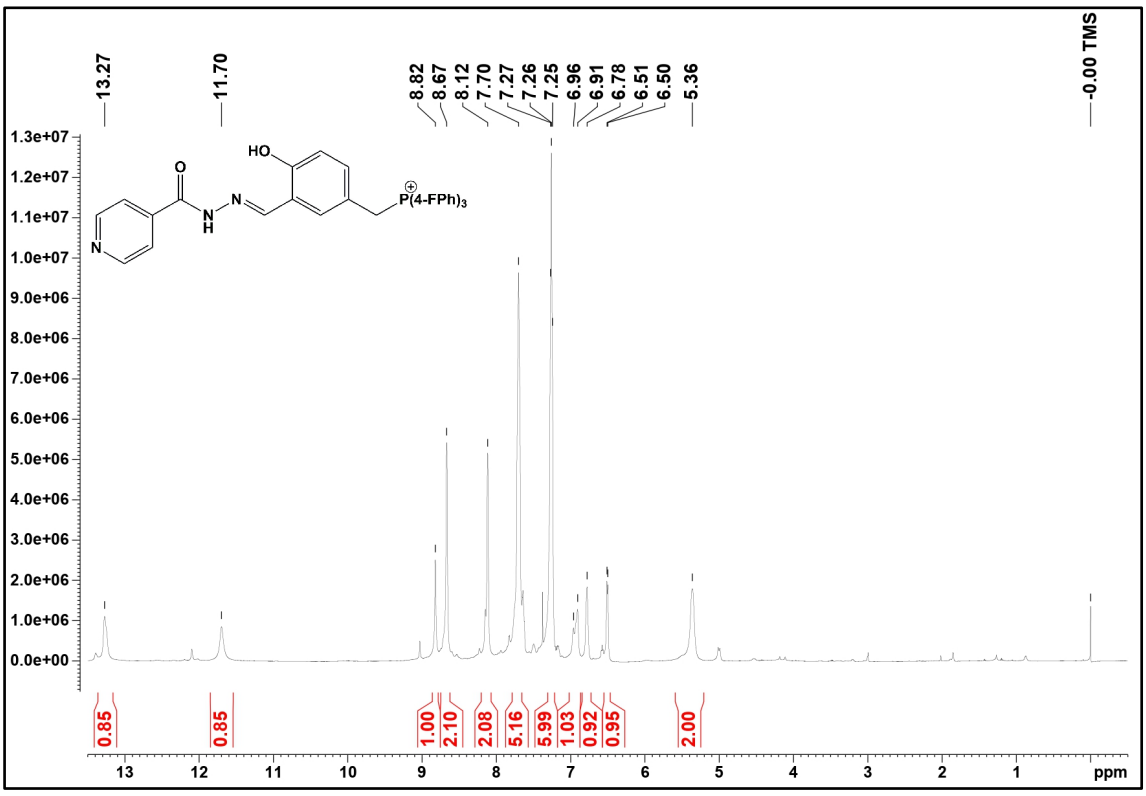

Fig. S22 ^{1}H-NMR spectra of **[H_2L2]Cl** (600 MHz, $CDCl_3$).

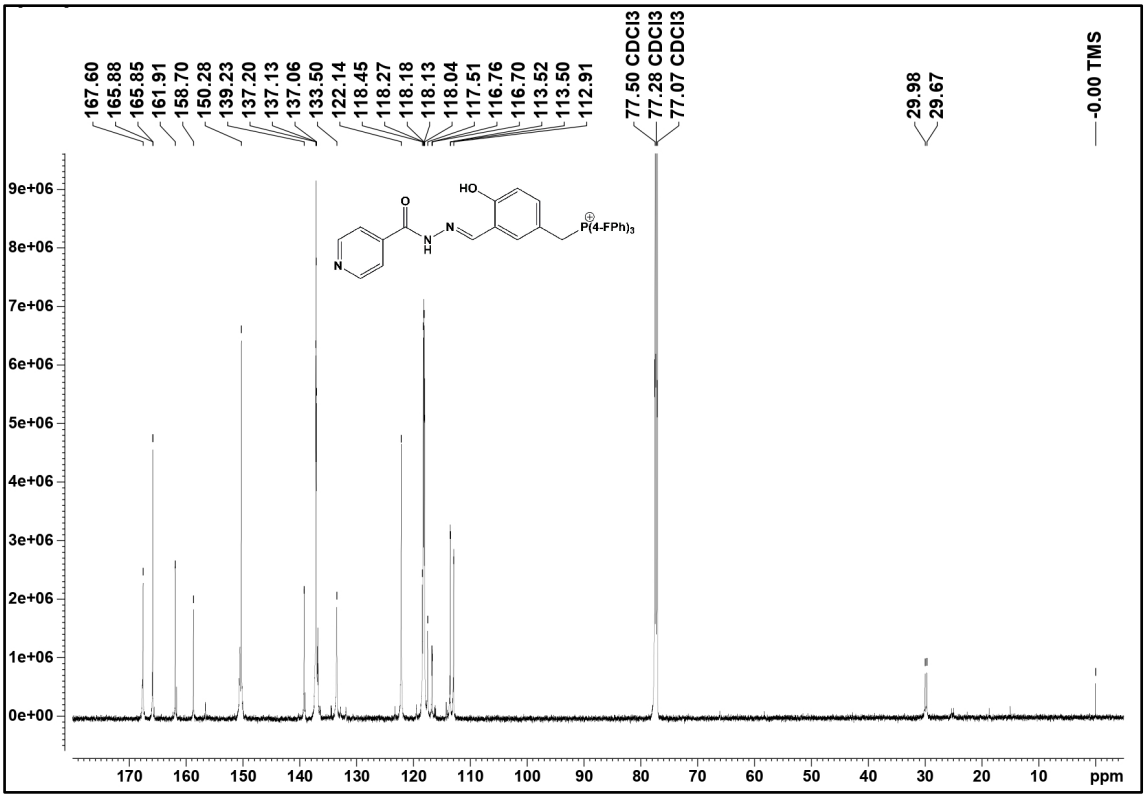

Fig. S23 ^{13}C-NMR spectra of **[H_2L2]Cl** (151 MHz, $CDCl_3$).

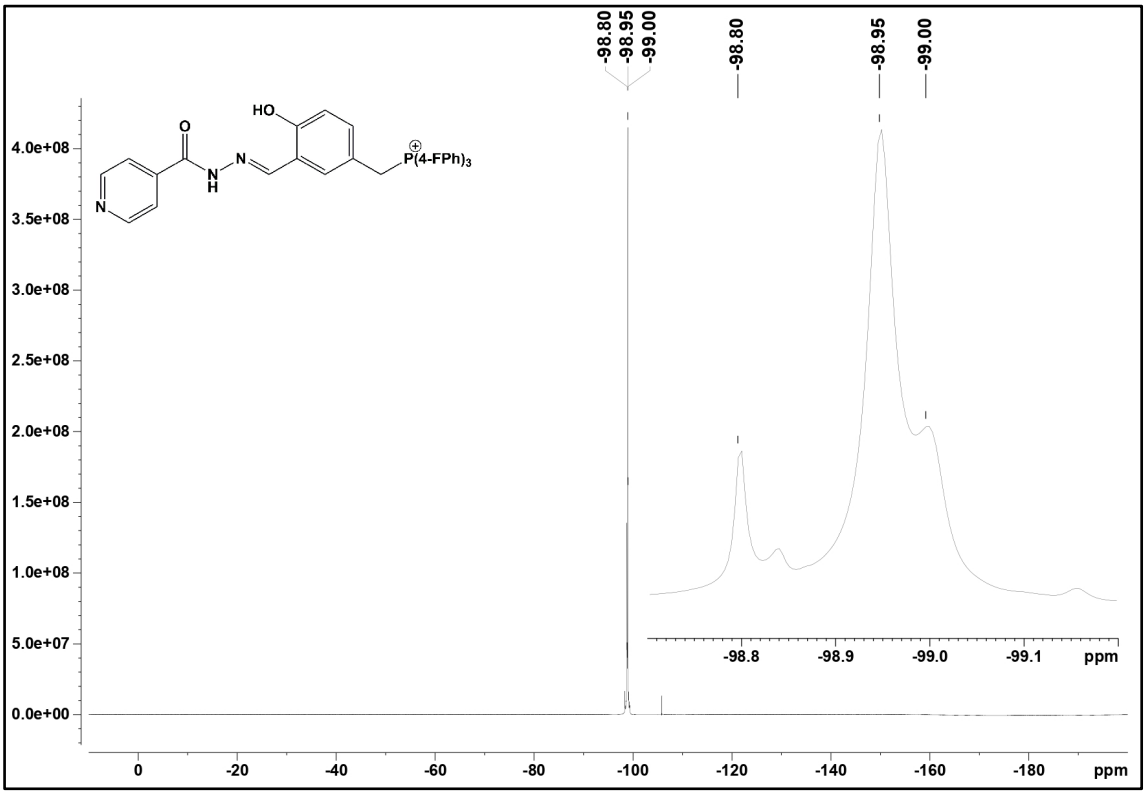

Fig. S24 ^{19}F-NMR spectra of **[H_2L2]Cl** (565 MHz, $CDCl_3$).

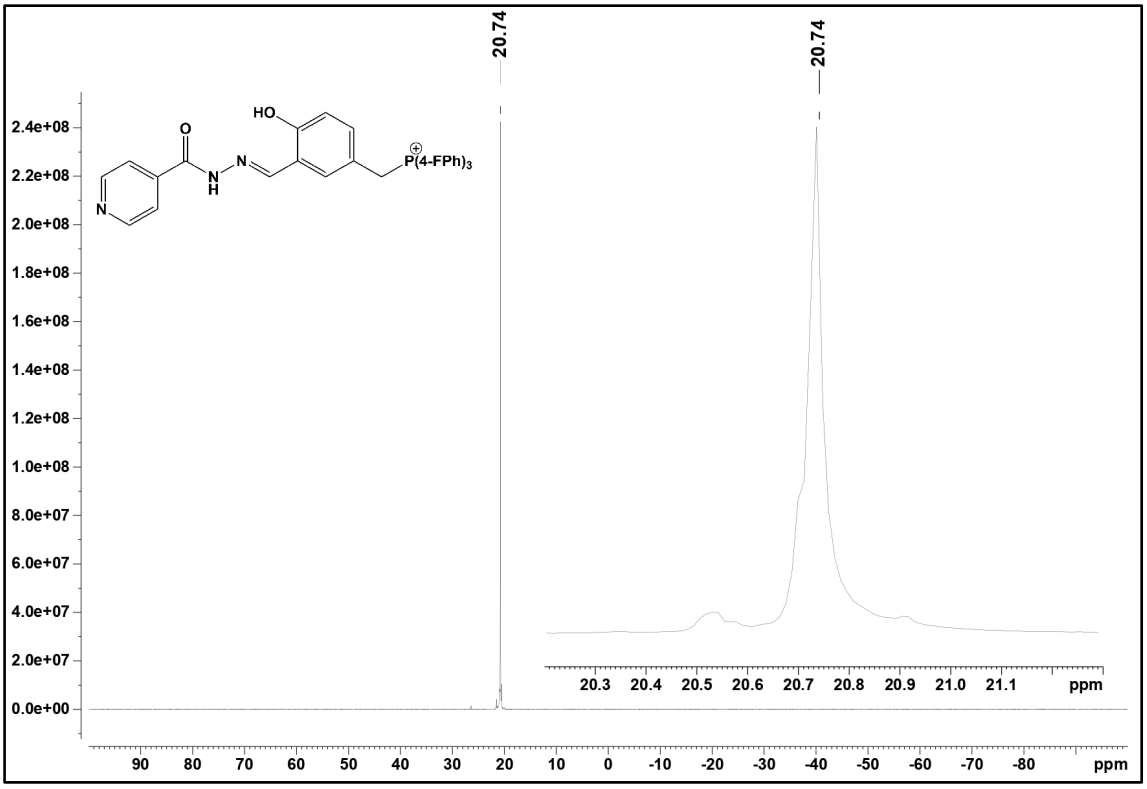

Fig. S25 ^{31}P-NMR spectra of **[H_2L2]Cl** (243 MHz, $CDCl_3$).

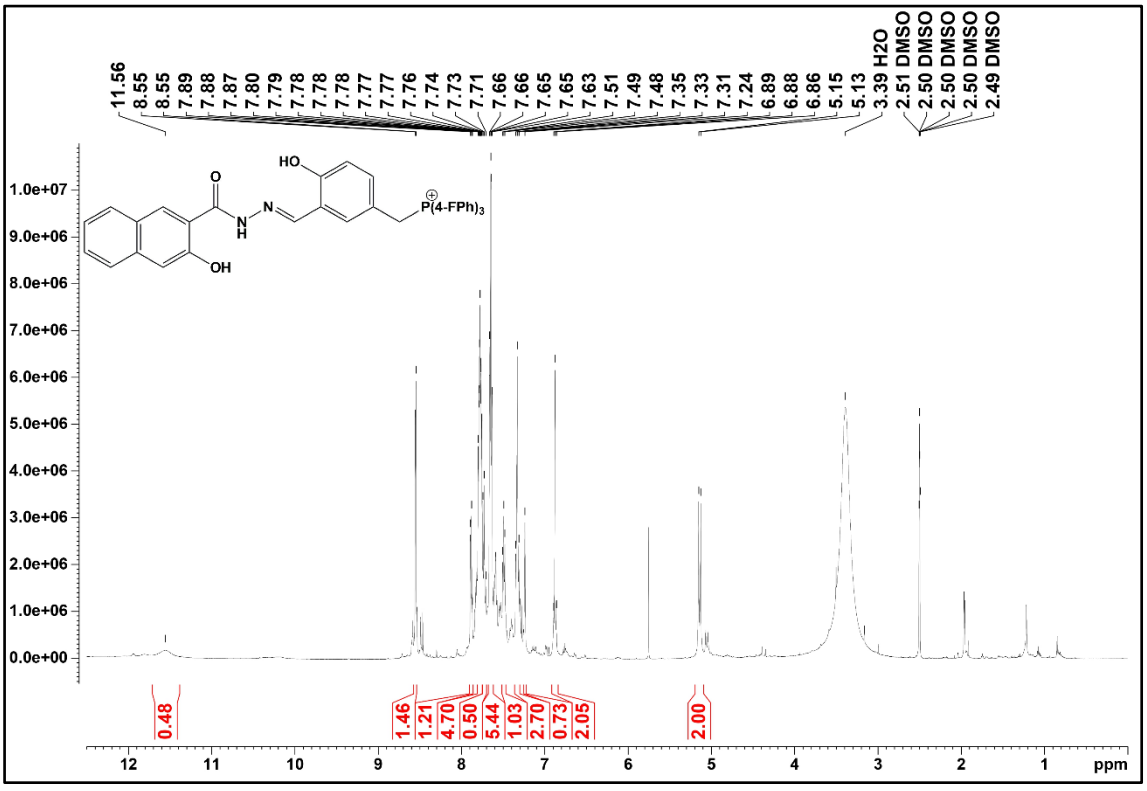

Fig. S26 ^{1}H-NMR spectra of **[H_3L3]Cl** (600 MHz, DMSO-d_6).

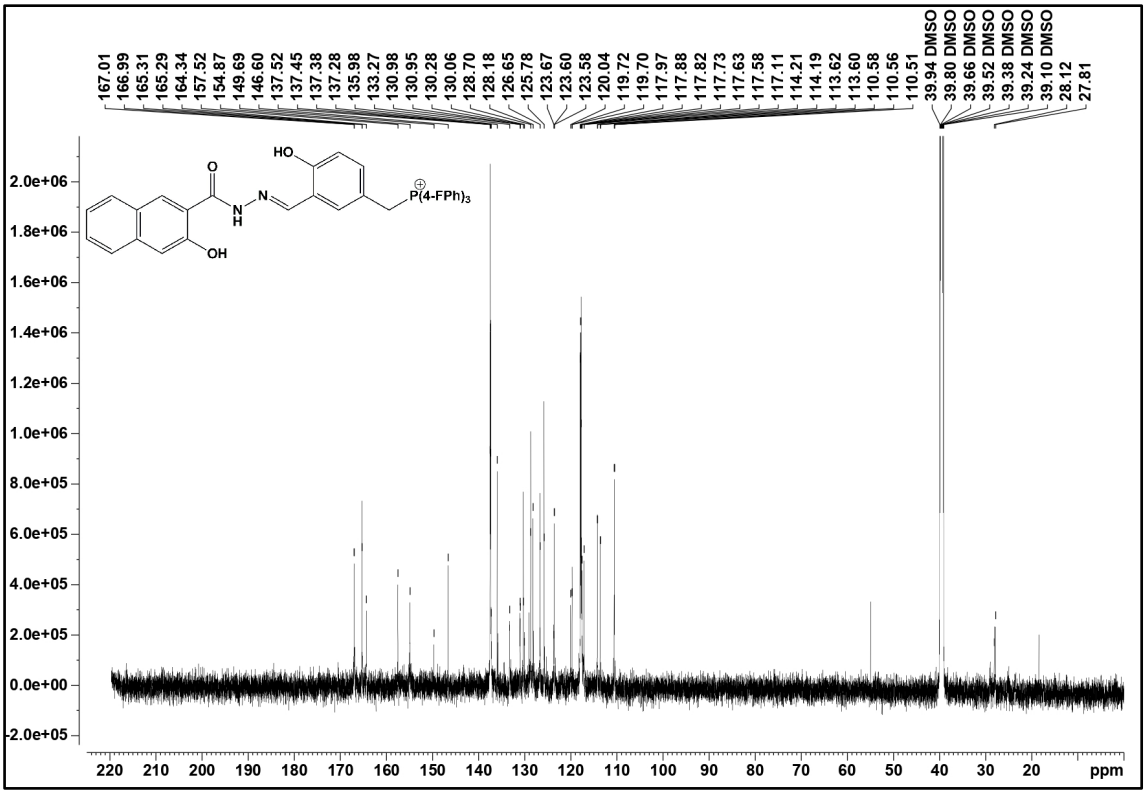

Fig. S27 ^{13}C-NMR spectra of **[H$_3$L3]Cl** (151 MHz, DMSO-d_6).

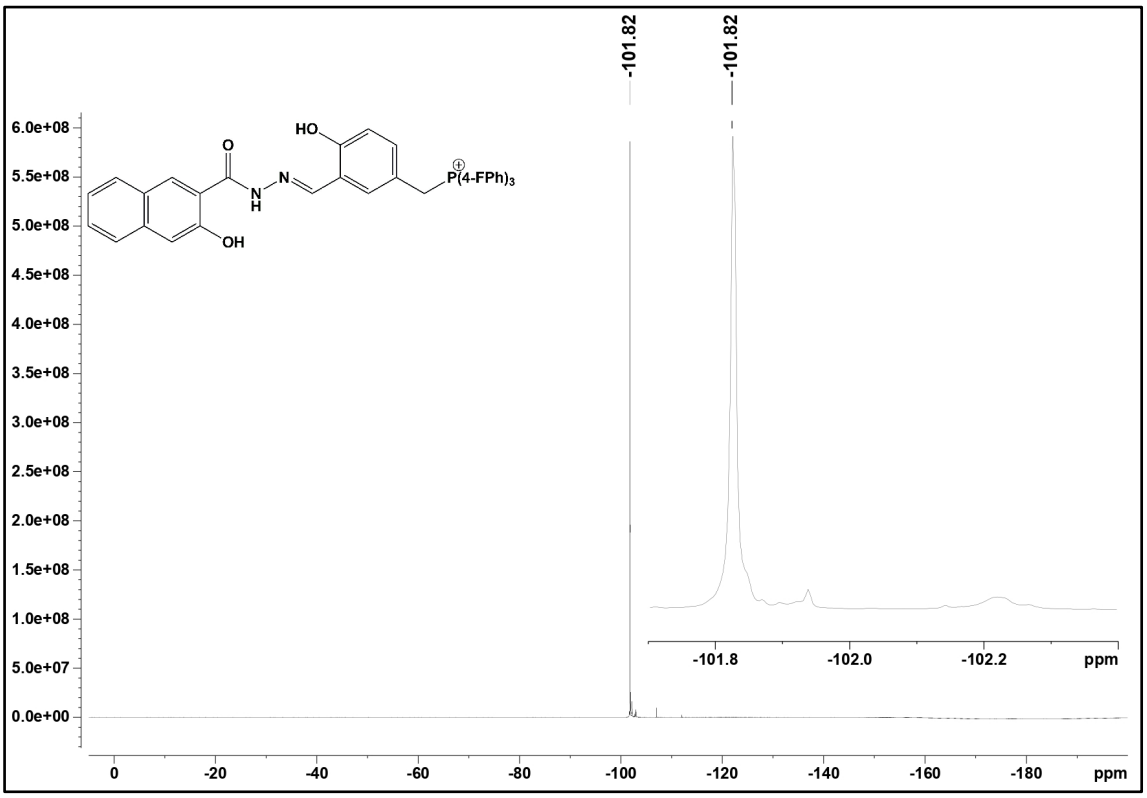

Fig. S28 ^{19}F-NMR spectra of **[H$_3$L3]Cl** (565 MHz, DMSO-d_6).

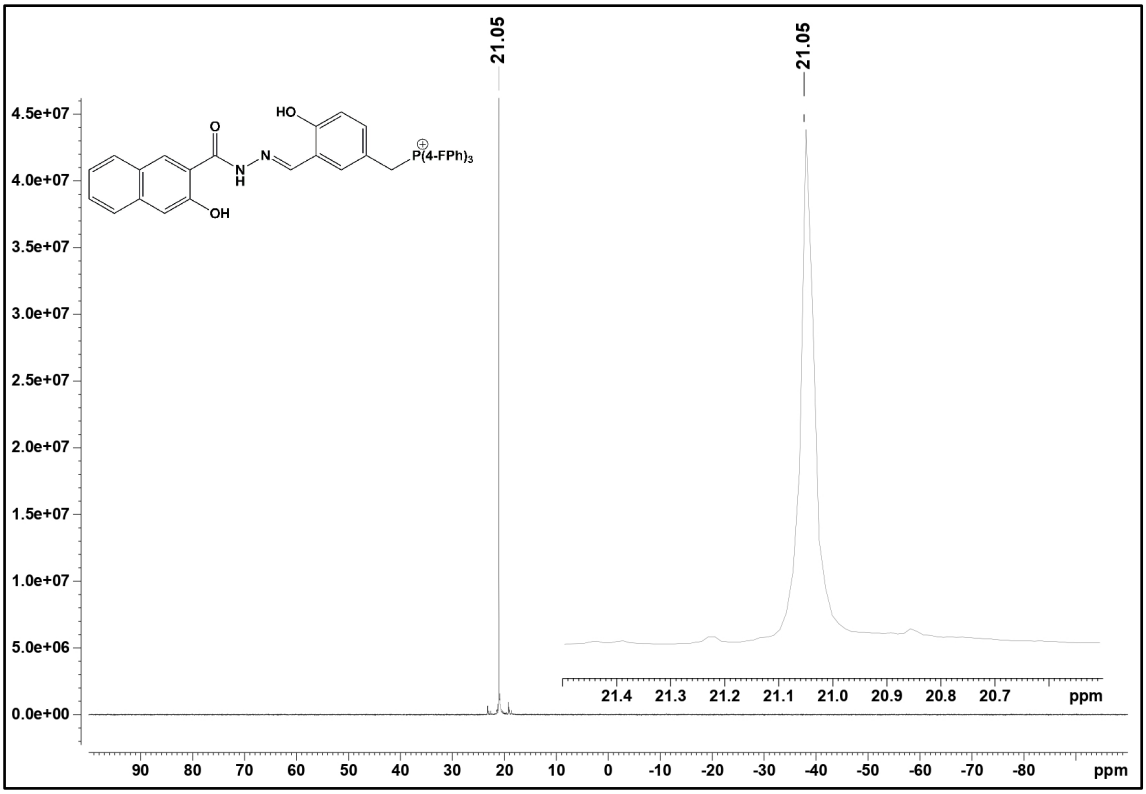

Fig. S29 ^{31}P-NMR spectra of **[H_3L3]Cl** (243 MHz, DMSO-d_6).

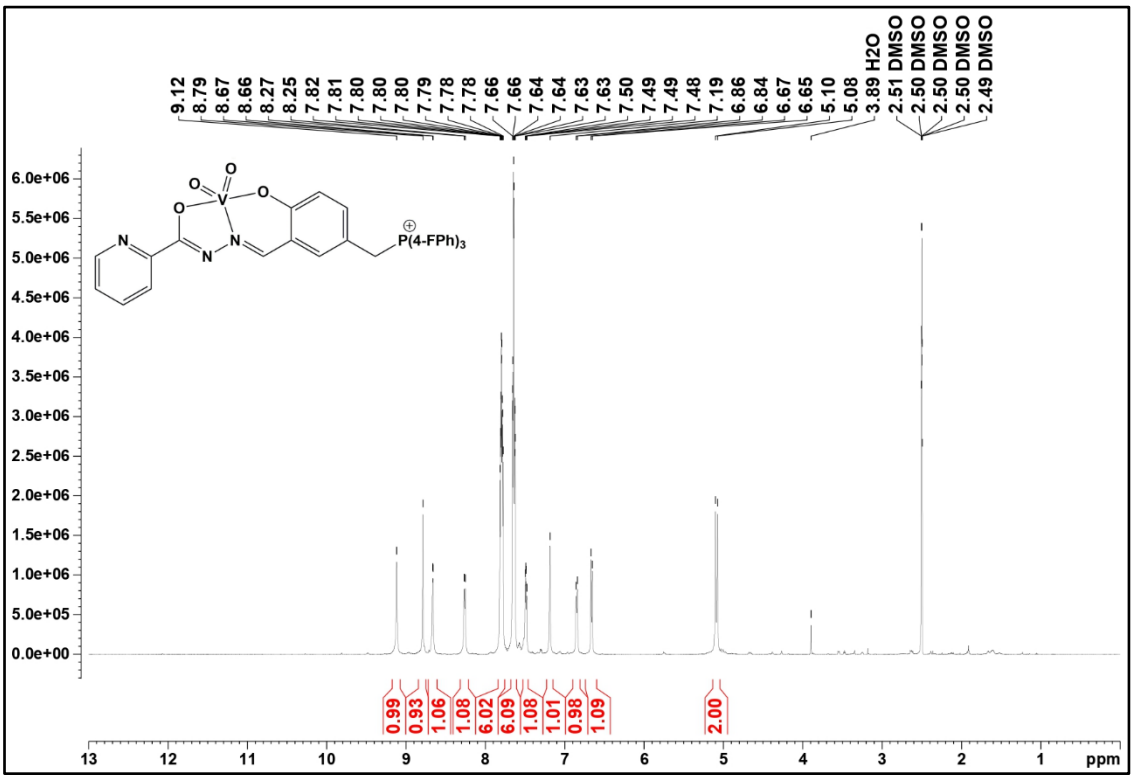

Fig. S30 ^{1}H-NMR spectra of $[VO_2L1]\cdot H_2O$ (**C1**) (600 MHz, DMSO-d_6).

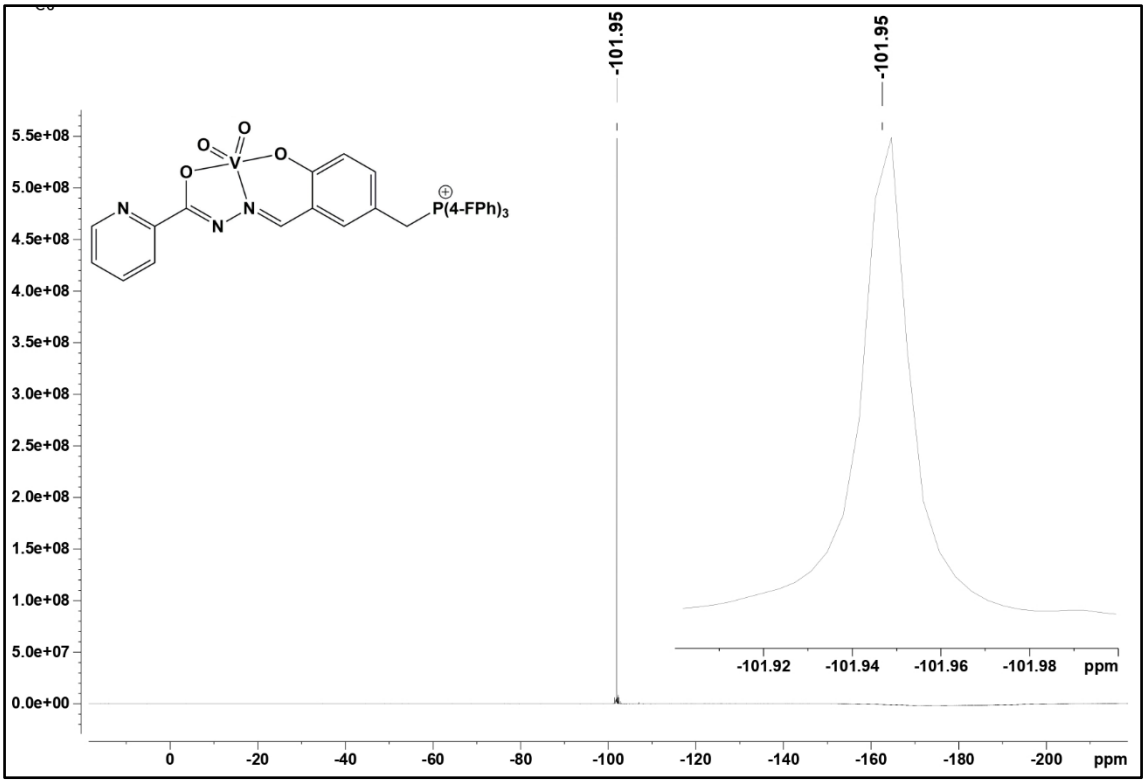

Fig. S31 ^{19}F-NMR spectra of $[VO_2L1]\cdot H_2O$ (**C1**) (565 MHz, DMSO-d_6).

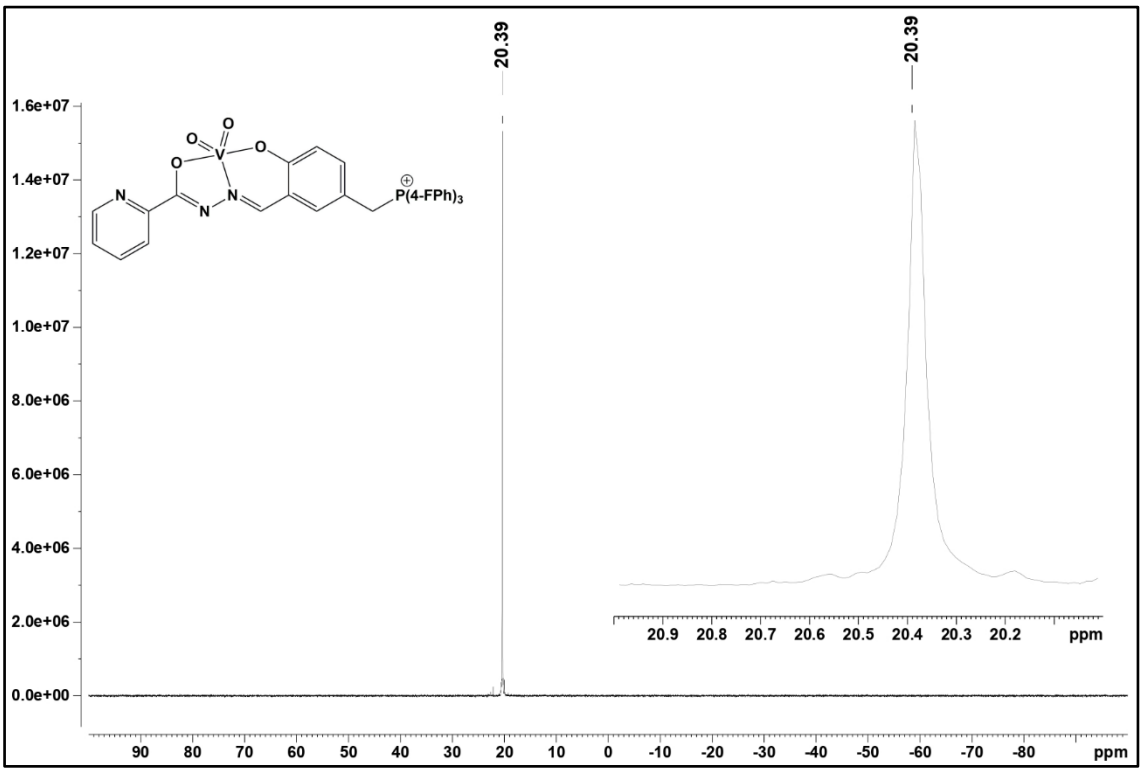

Fig. S32 ^{31}P-NMR spectra of $[VO_2L1]\cdot H_2O$ (**C1**) (243 MHz, DMSO-d_6).

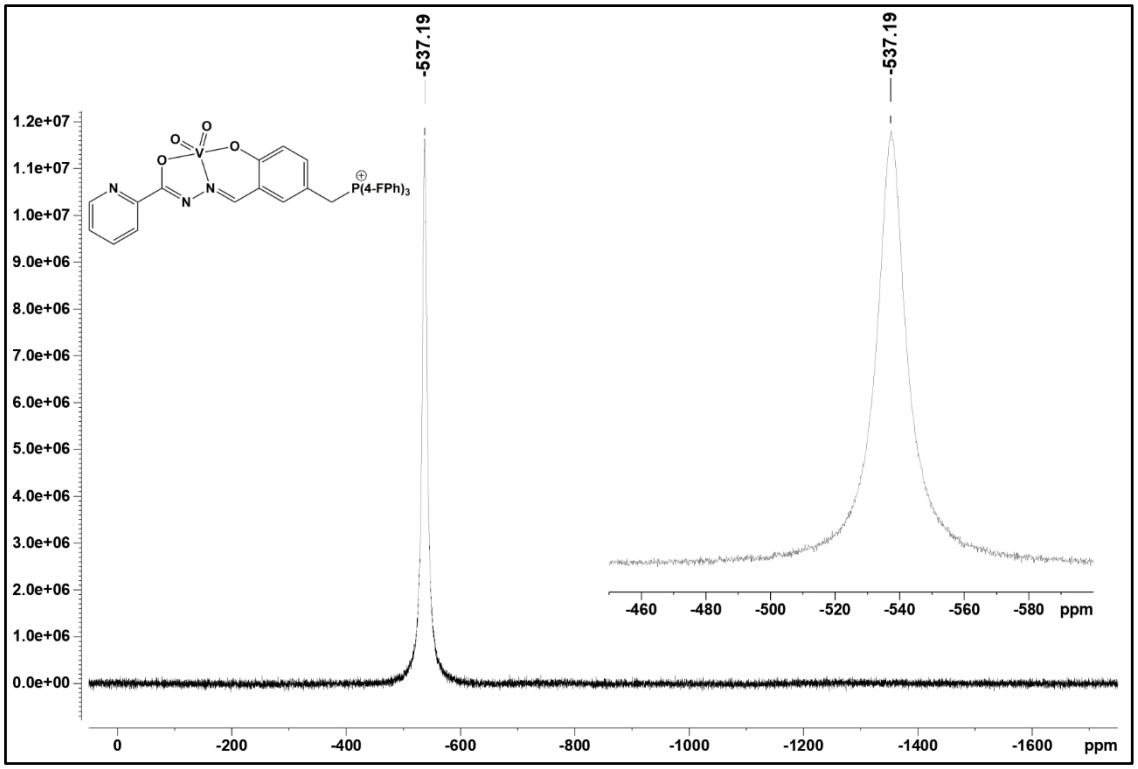

Fig. S33 ^{51}V-NMR spectra of $[VO_2L1]\cdot H_2O$ (**C1**) (158 MHz, DMSO-d_6).

Fig. S34 ^{1}H-NMR spectra of $[VO_2L2]\cdot CH_3OH$ (**C2**) (600 MHz, DMSO-d_6)

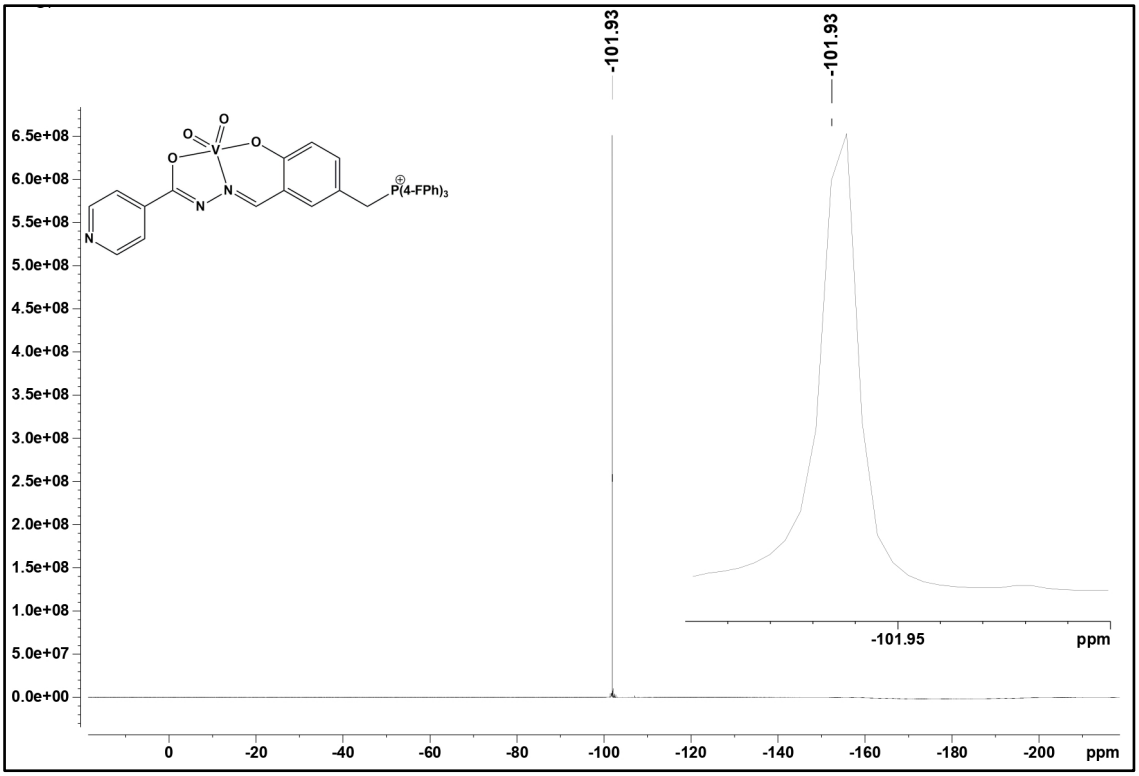

Fig. S35 ^{19}F-NMR spectra of $[VO_2L2]\cdot CH_3OH$ (**C2**) (565 MHz, DMSO-d_6).

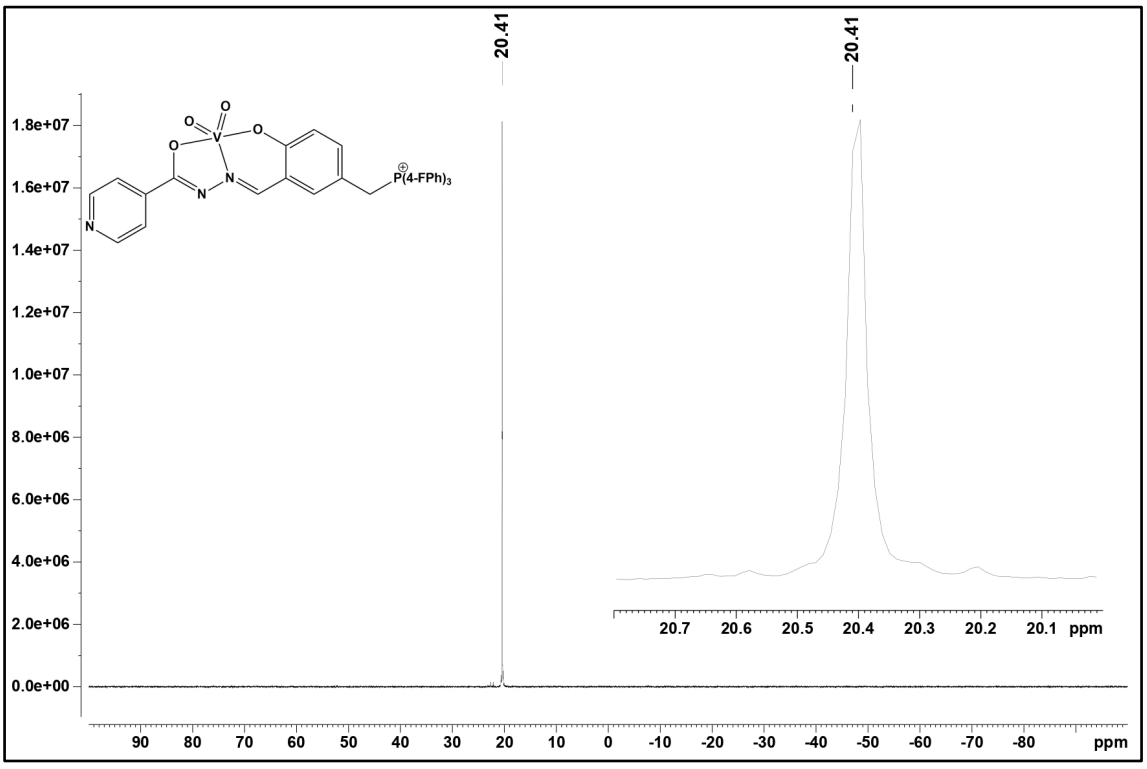

Fig. S36^{31}P-NMR spectra of $[VO_2L2]\cdot CH_3OH$ (**C2**) (243 MHz, DMSO-d_6)

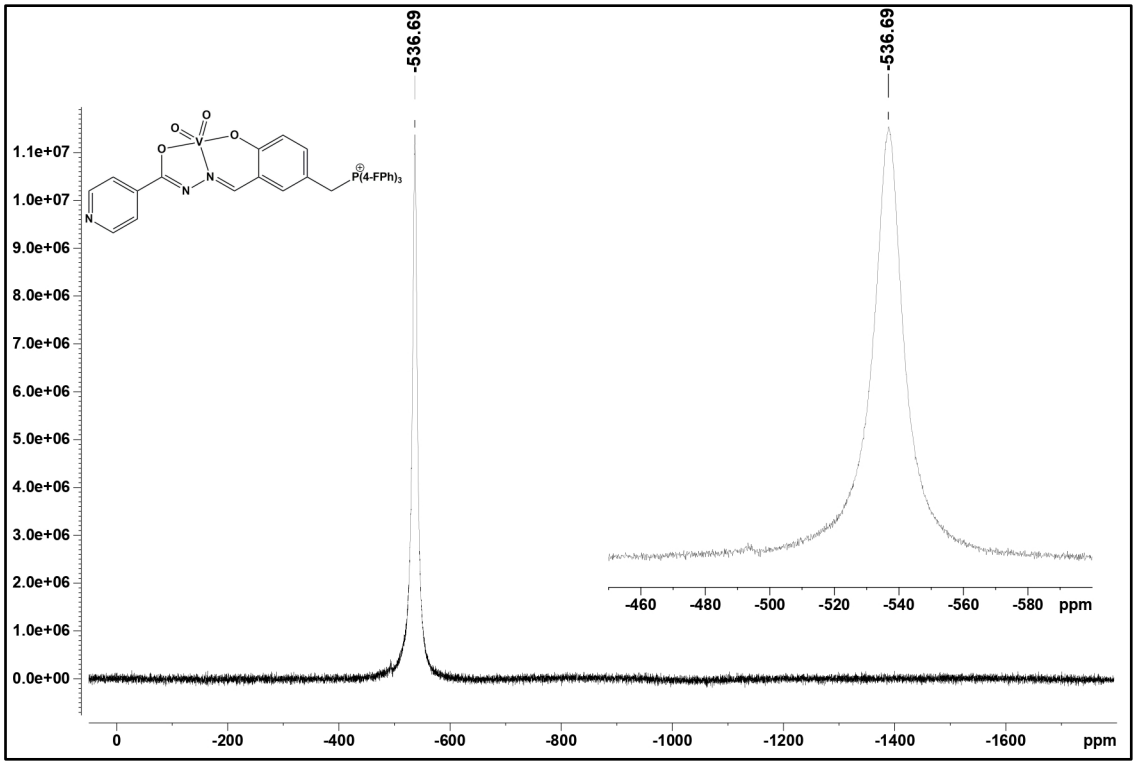

Fig. S37 ^{51}V-NMR spectra of $[VO_2L2]\cdot CH_3OH$ (**C2**) (158 MHz, DMSO-d_6).

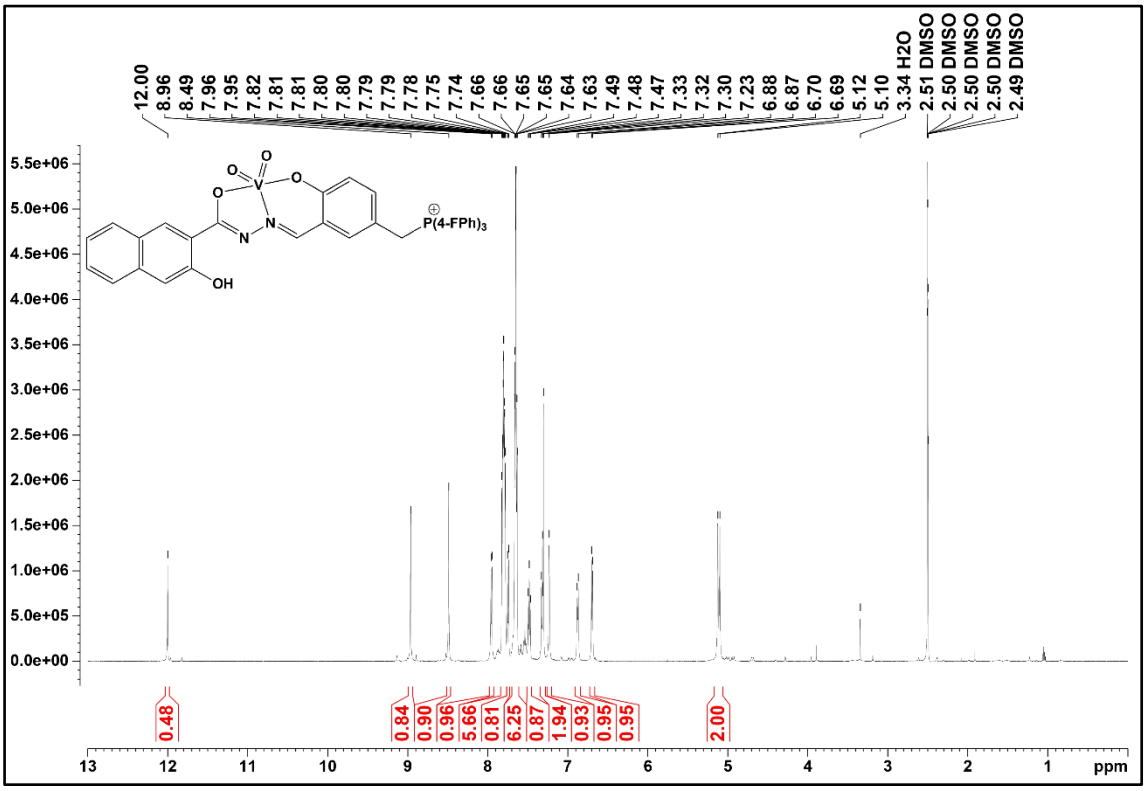

Fig. S38 ^{1}H-NMR spectra of $[VO_2HL3]\cdot CH_3OH\cdot H_2O$ (**C3**) (600 MHz, DMSO-d_6).

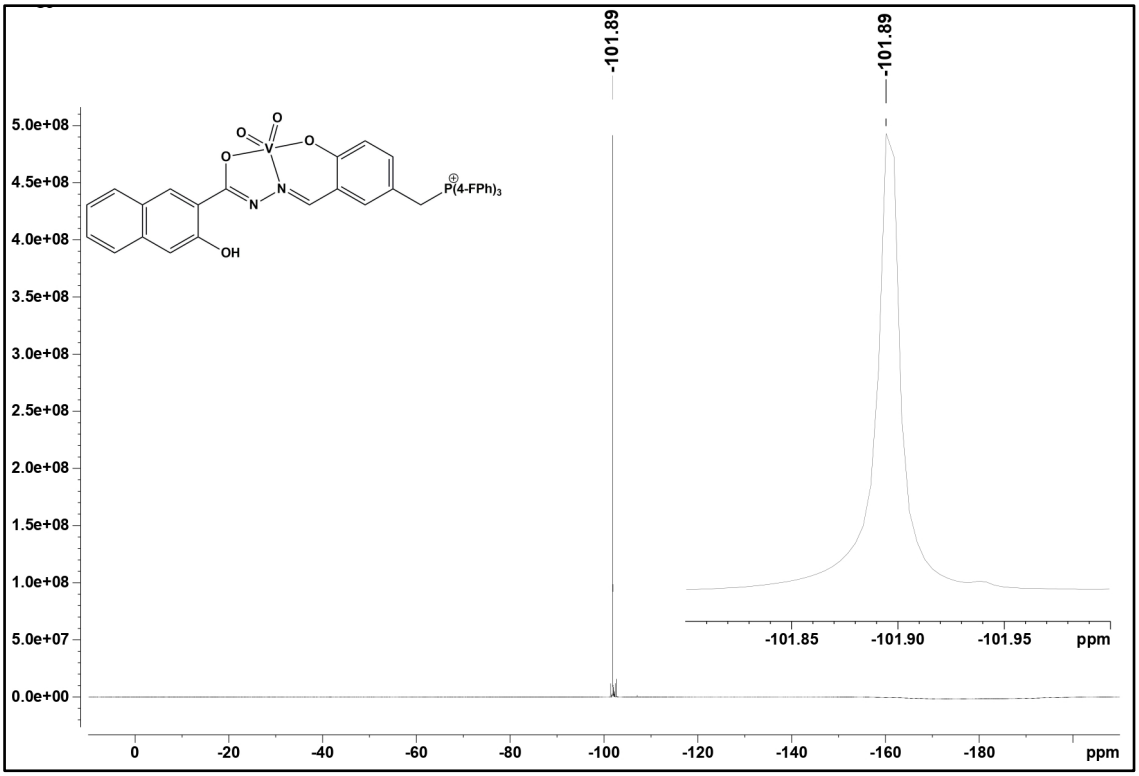

Fig. S39 ^{19}F-NMR spectra of $[VO_2HL3]\cdot CH_3OH\cdot H_2O$ (**C3**) (565 MHz, DMSO-d_6).

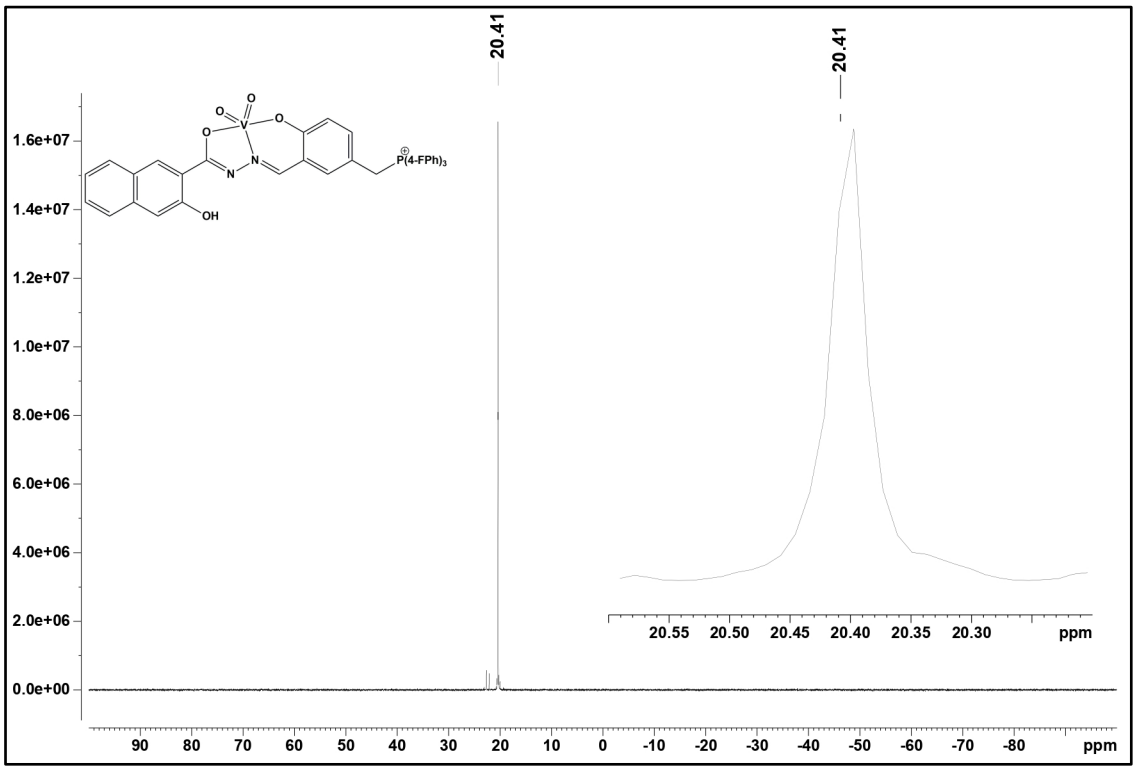

Fig. S40 ^{31}P-NMR spectra of $[VO_2HL3]\cdot CH_3OH\cdot H_2O$ (**C3**) (243 MHz, DMSO-d_6).

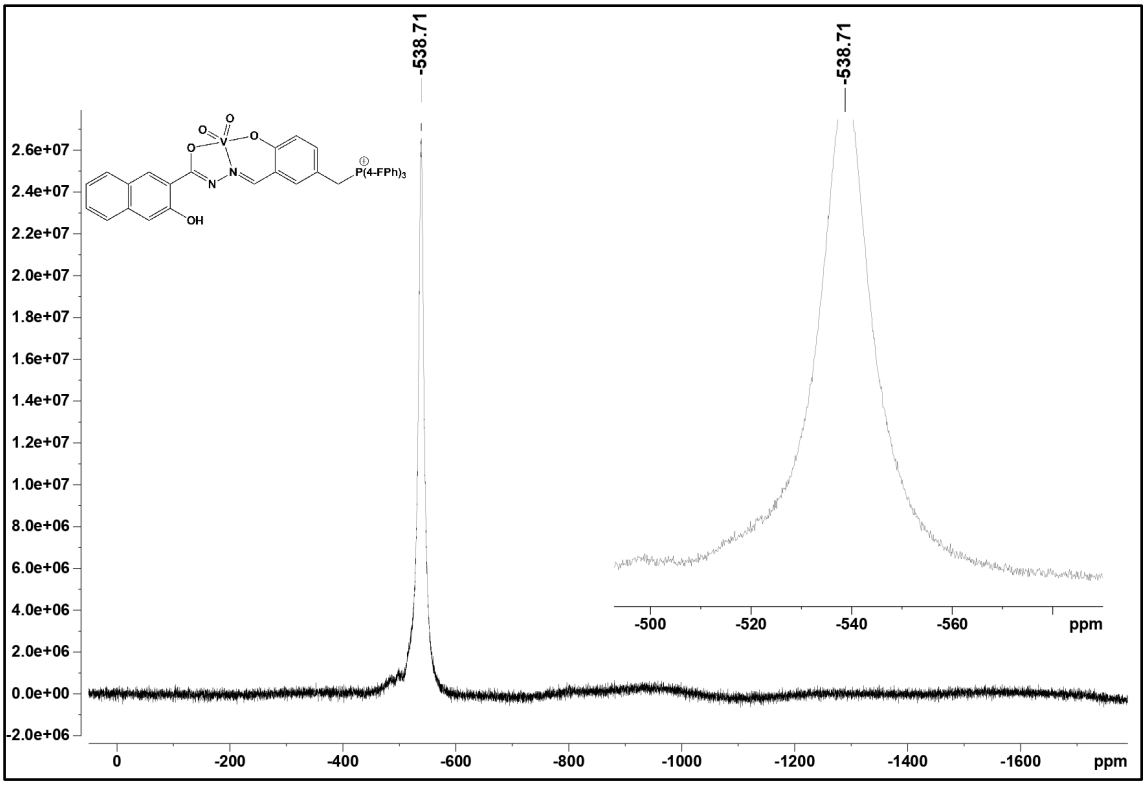

Fig. S41 ^{51}V-NMR spectra of $[VO_2HL3]\cdot CH_3OH\cdot H_2O$ (**C3**) (158 MHz, DMSO-d_6).

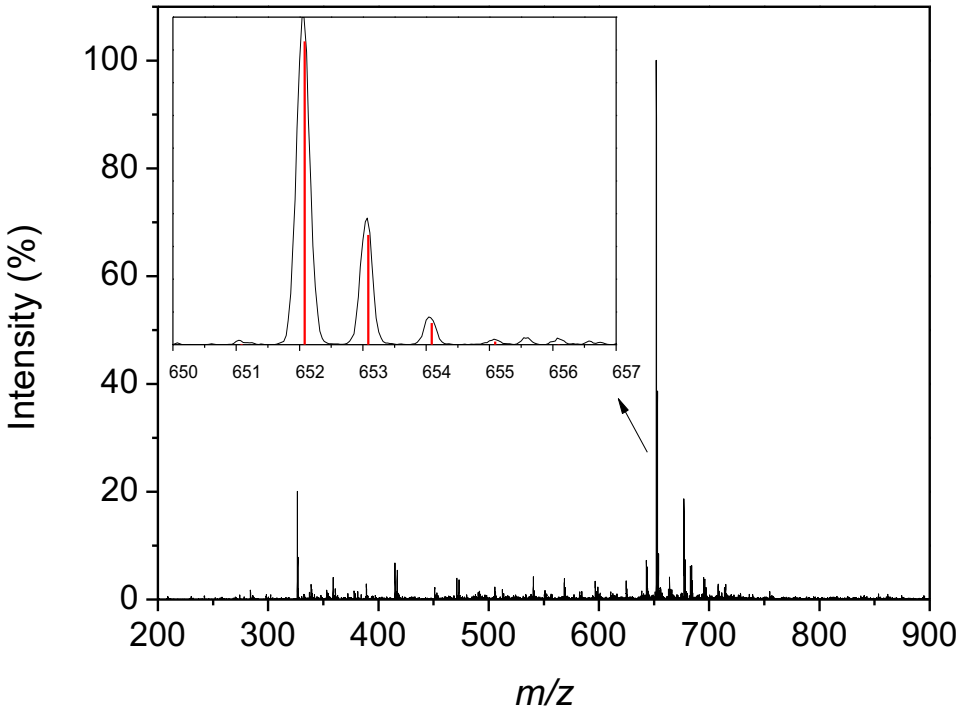

Fig. S42 ESI-MS spectrum (positive mode) in acetonitrile of complex **C1**.

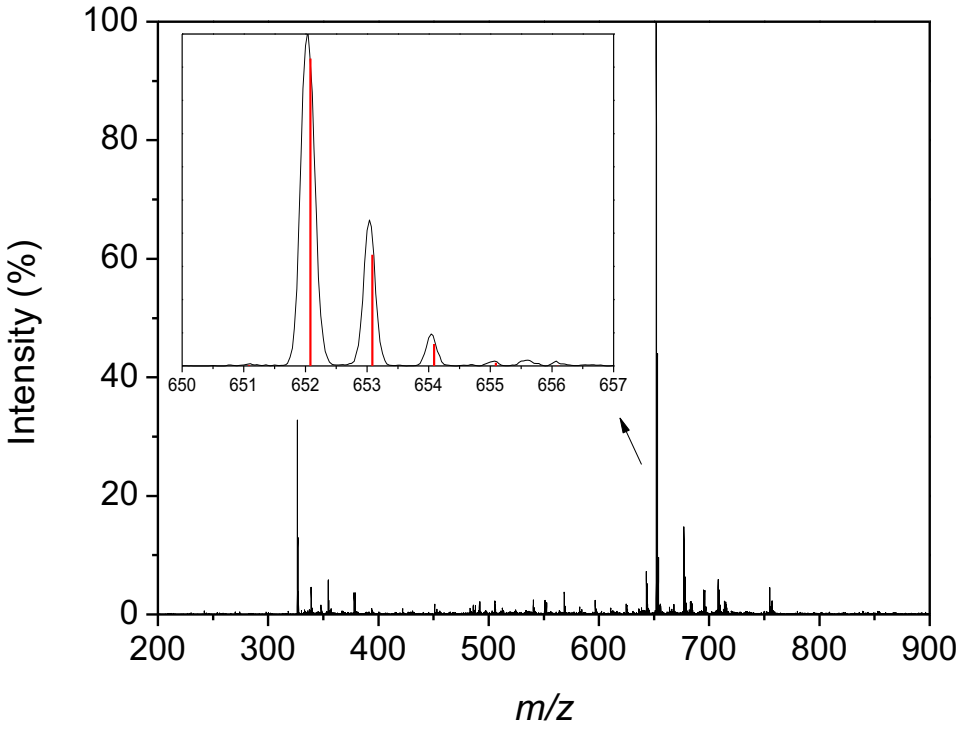

Fig. S43 ESI-MS spectrum (positive mode) in acetonitrile of complex **C2**.

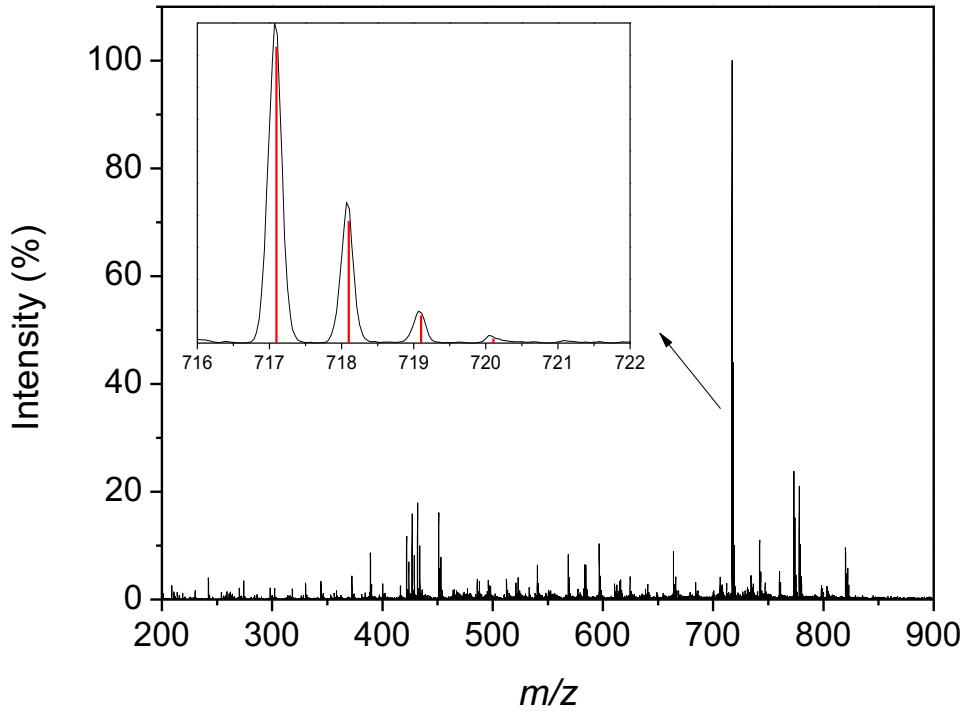

Fig. S44 ESI-MS spectrum (positive mode) in acetonitrile of complex **C3**.

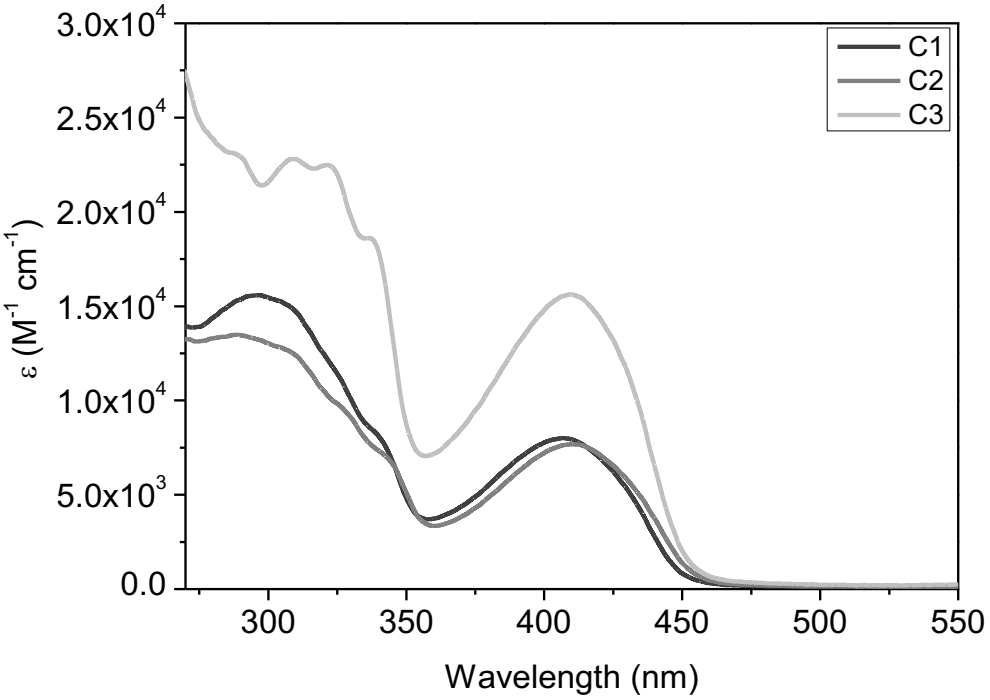

Fig. S45 UV-Vis spectra of complexes **C1-C3** in *N*,*N*-Dimethylformamide (DMF) solution ([**C**]=3 × 10^{-5} M).

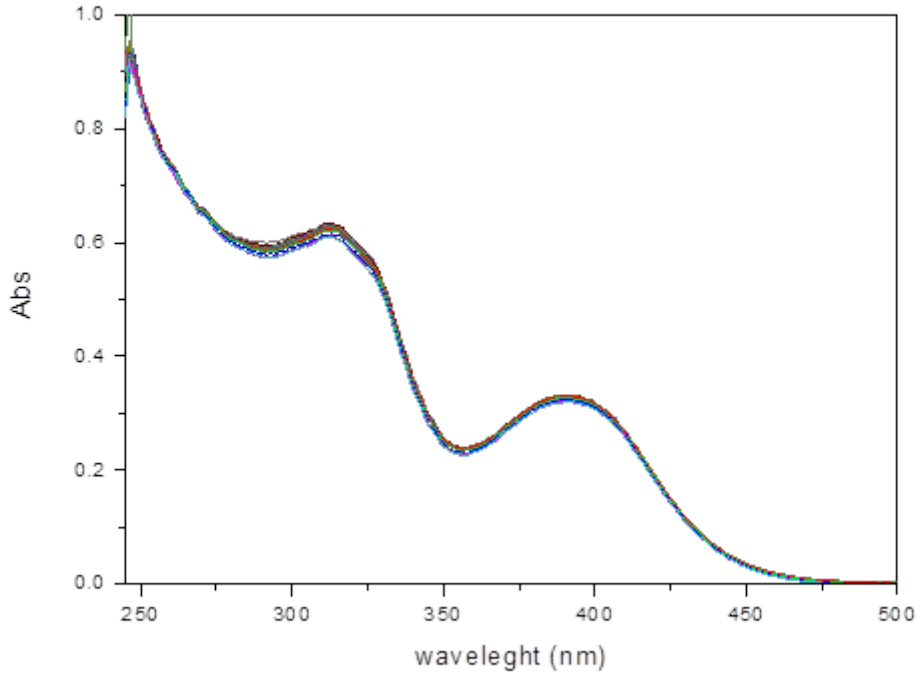

Fig. S46 UV-vis spectra for **C1** (3×10^{-5} M) in DMF/buffer (TRIS 0.5 mM) 5% v/v; pH 7.40, *I* = 0.5 mM (NaCl); 25 °C, over 24 h.

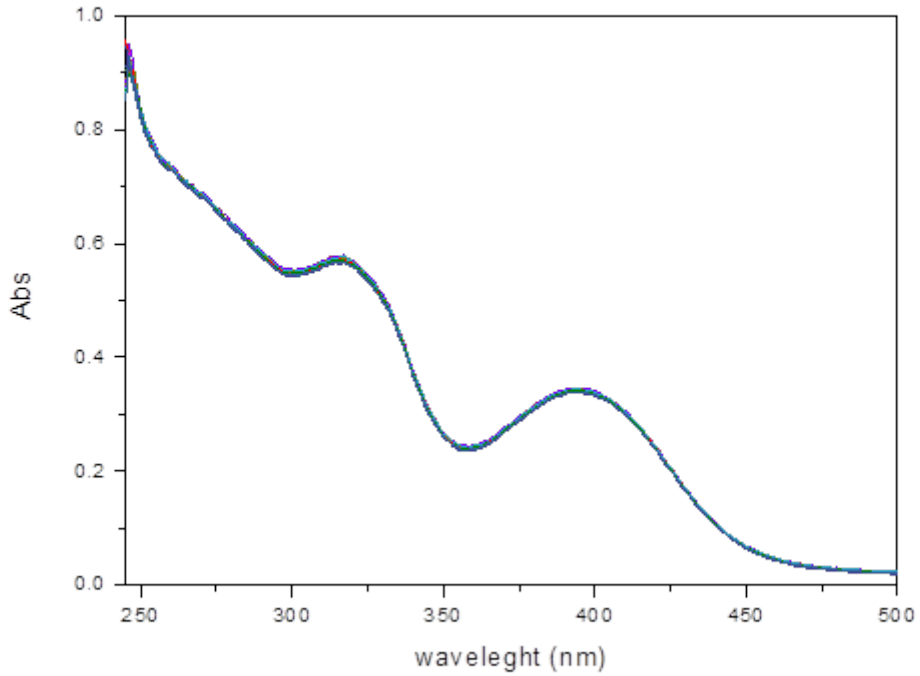

Fig. S47 UV-vis spectra for **C2** (3×10^{-5} M) in DMF/buffer (TRIS 0.5 mM) 5% v/v; pH 7.40, *I* = 0.5 mM (NaCl); 25 °C, over 24 h.

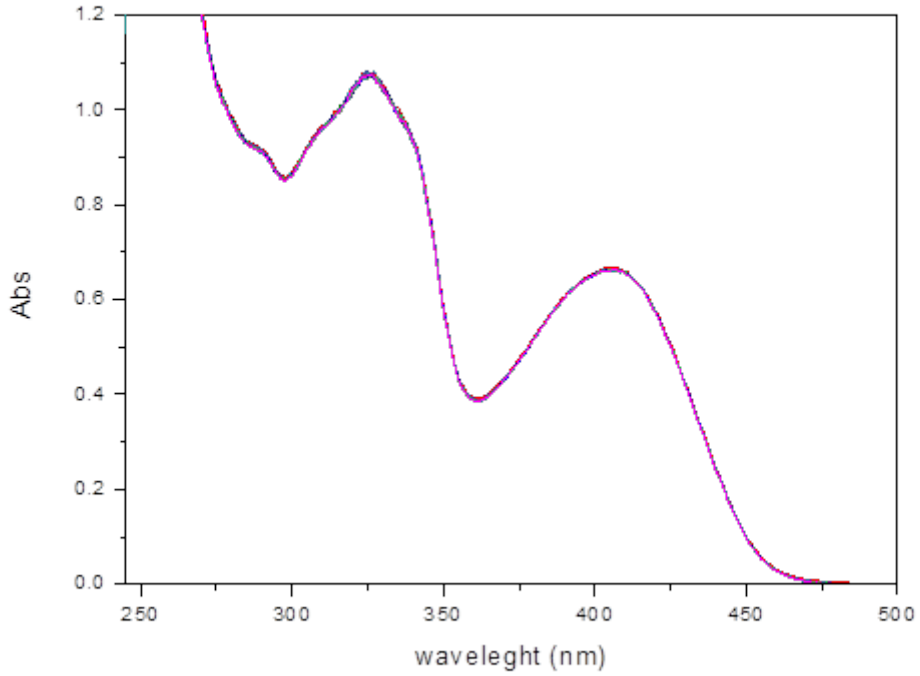

Fig. S48 UV-vis spectra for **C3** (3×10^{-5} M) in DMF/buffer (TRIS 0.5 mM) 5% v/v; pH 7.40, *I* = 0.5 mM (NaCl); 25 °C, over 24 h.

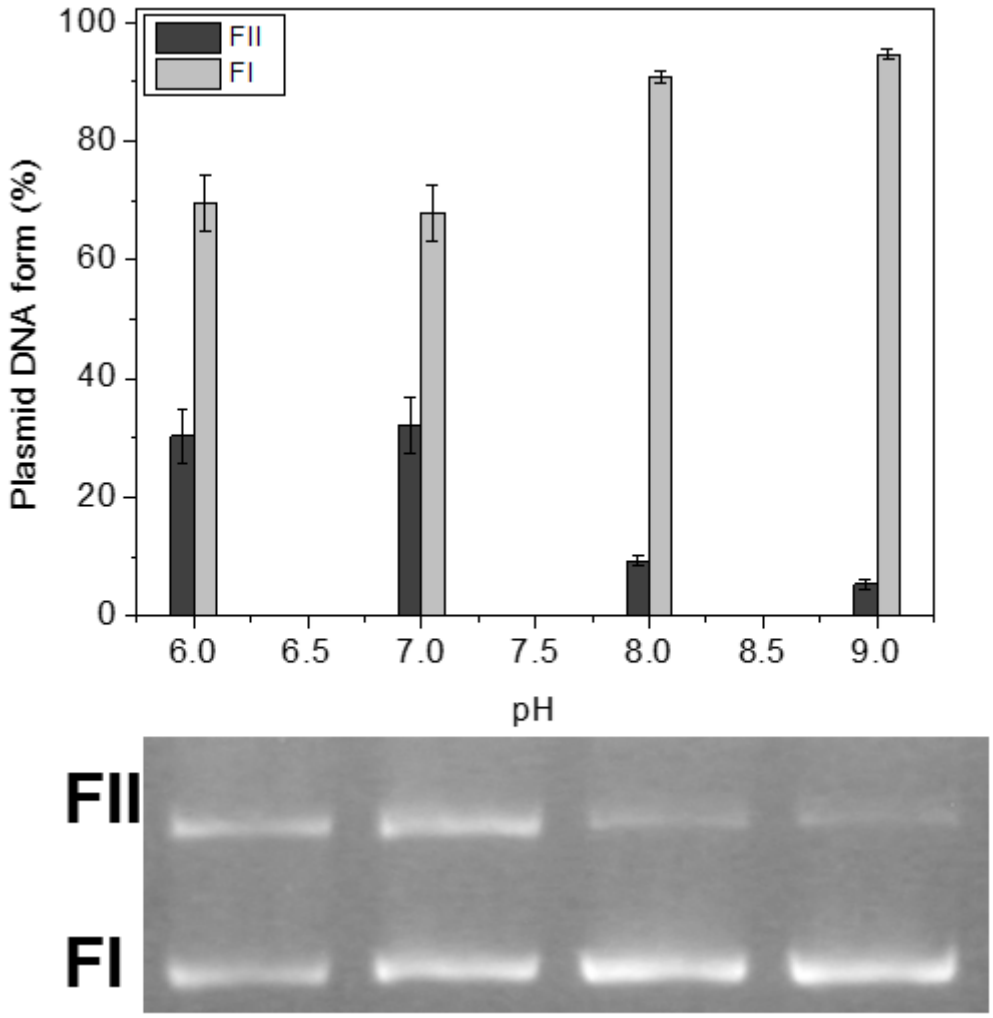

Fig. S49 pH effect on plasmid DNA cleavage with complex **C1**. Experimental conditions: [DNA] = 330 ng, ~25 μM; [Buffer] = 10 mM, MES (6.0); HEPES (pH 7.0); HEPES (8.0); CHES (9.00); Complexes concentration = 500 μM; Temperature = 50 °C; Incubation time = 8 hours sheltered from light.

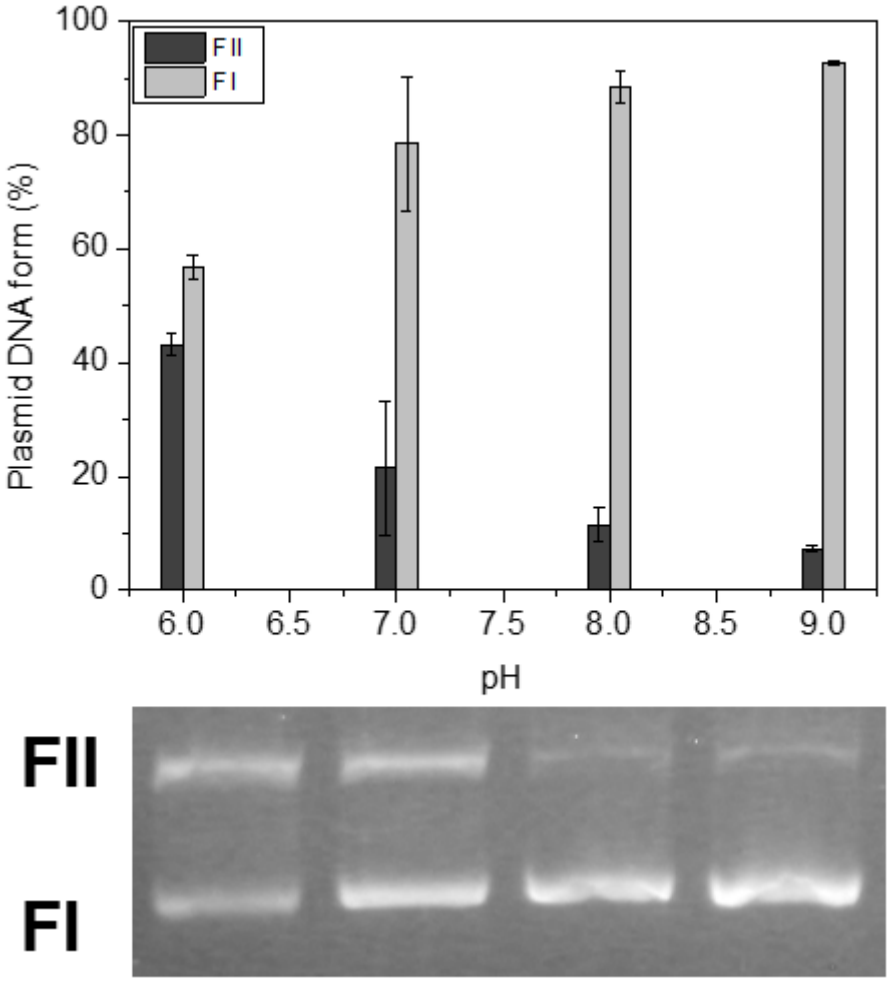

Fig. S50 pH effect on plasmid DNA cleavage with complex **C2**. Experimental conditions: [DNA] = 330 ng, ~25 μM; [Buffer] = 10 mM, MES (6.0); HEPES (pH 7.0); HEPES (8.0); CHES (9.00); Complexes concentration = 500 μM; Temperature = 50 °C; Incubation time = 8 hours sheltered from light.

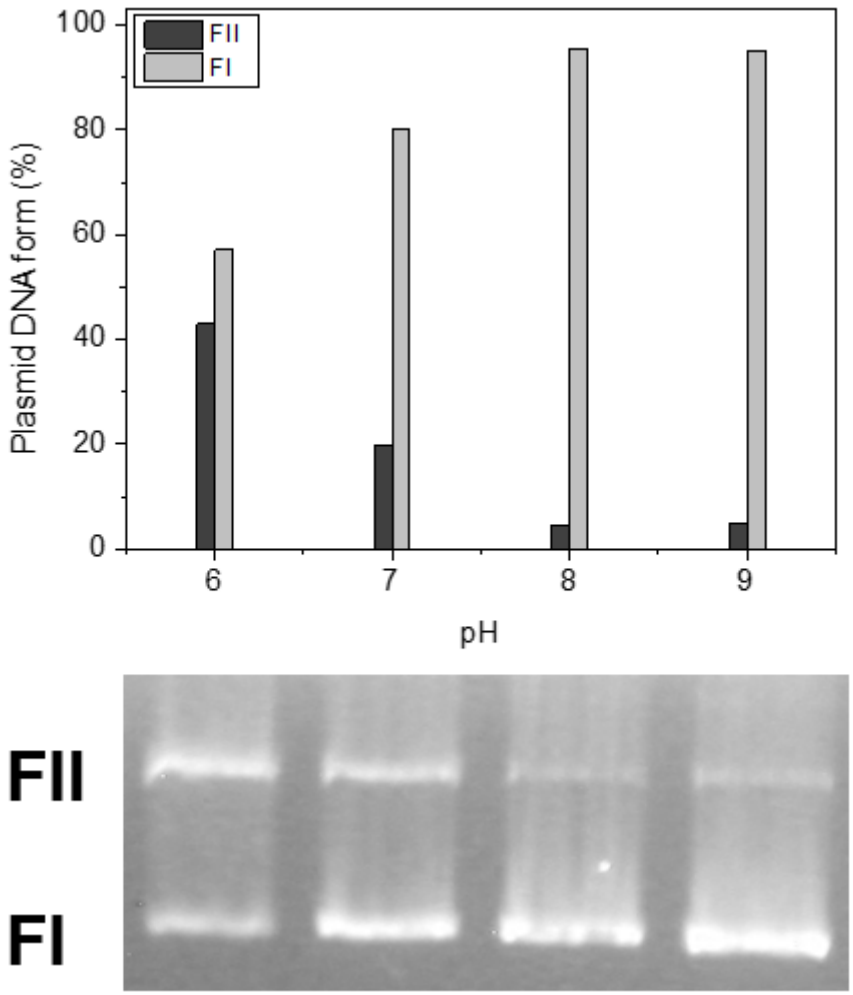

Fig. S51 pH effect on plasmid DNA cleavage with complex **C3**. Experimental conditions: [DNA] = 330 ng, ~25 μM; [Buffer] = 10 mM, MES (6.0); HEPES (pH 7.0); HEPES (8.0); CHES (9.00); Complexes concentration = 500 μM; Temperature = 50 °C; Incubation time = 8 hours sheltered from light.

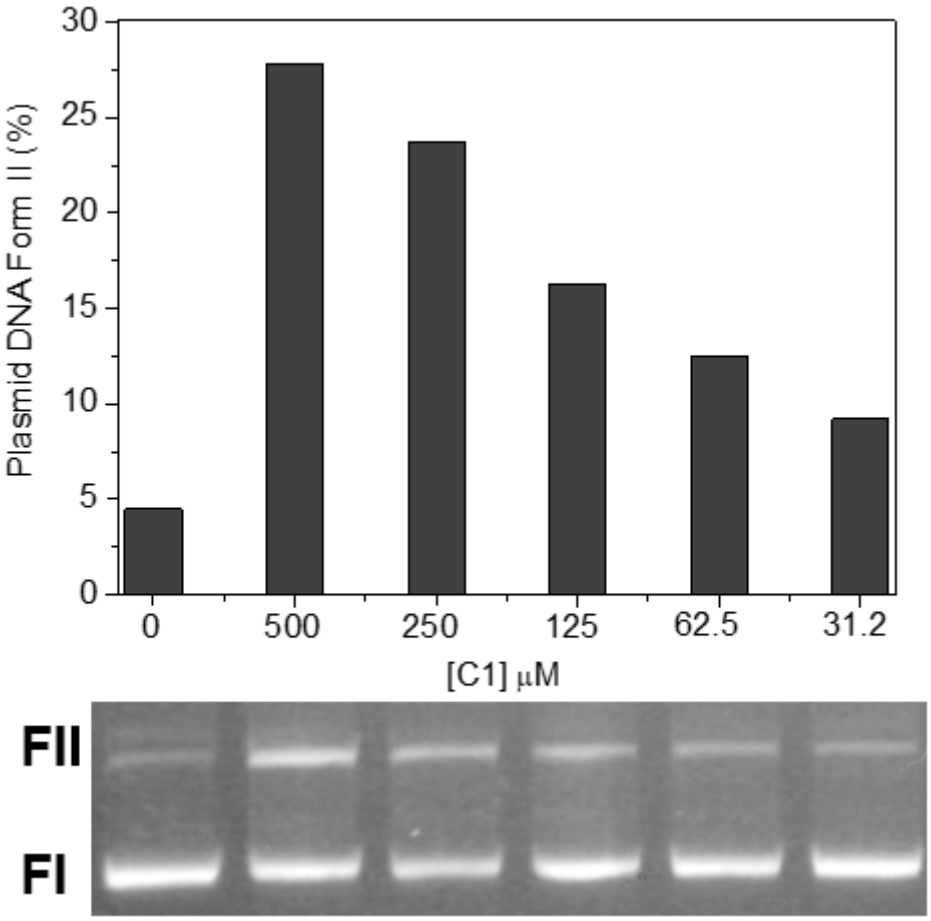

Fig. S52 Complex **C1** concentration effect on plasmid DNA cleavage. Experimental conditions: [DNA] = 330 ng, ~25 μM; [Buffer] = 10 mM, HEPES (pH 7.0); Complex concentration = 500 - 0 μM; Temperature = 50 °C; Incubation time = 8 hours sheltered from light.

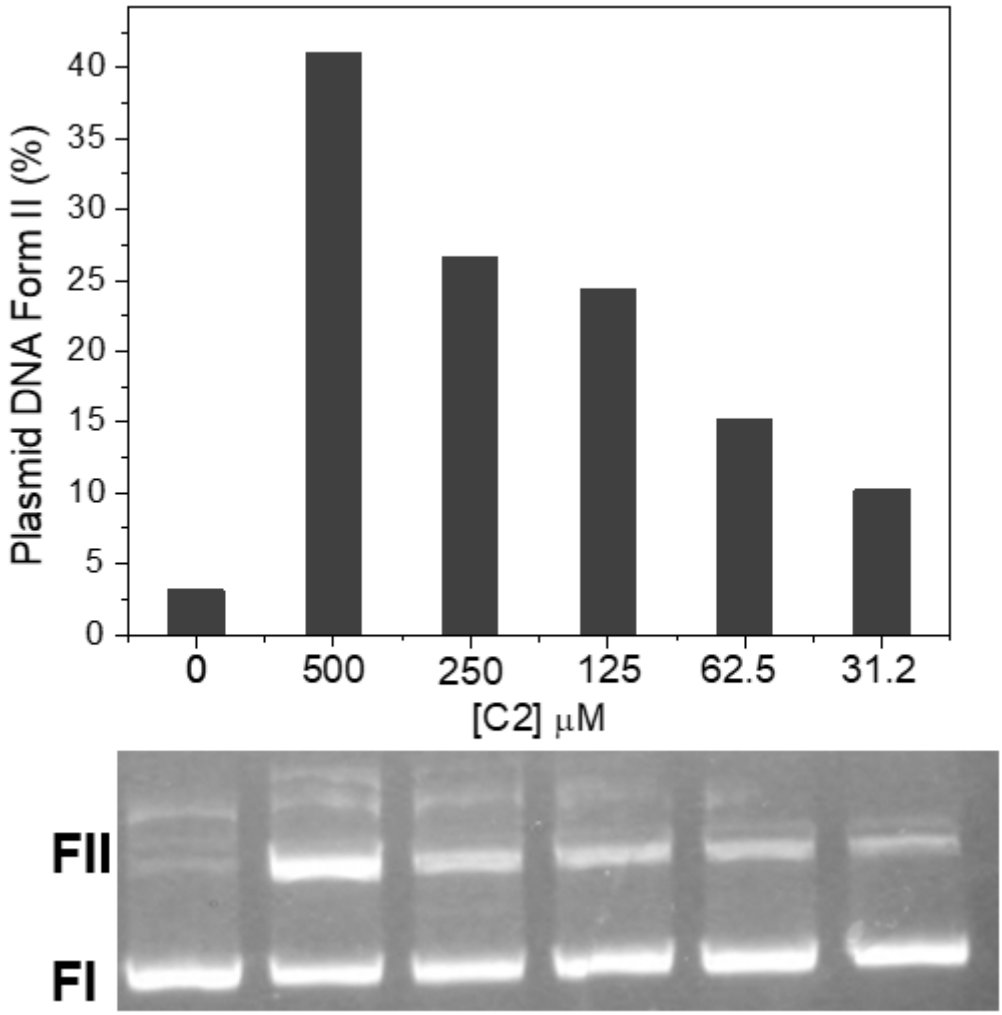

Fig. S53 Complex **C2** concentration effect on plasmid DNA cleavage. Experimental conditions: [DNA] = 330 ng, ~25 μM; [Buffer] = 10 mM, HEPES (pH 7.0); Complex concentration = 500 - 0 μM; Temperature = 50 °C; Incubation time = 8 hours sheltered from light.

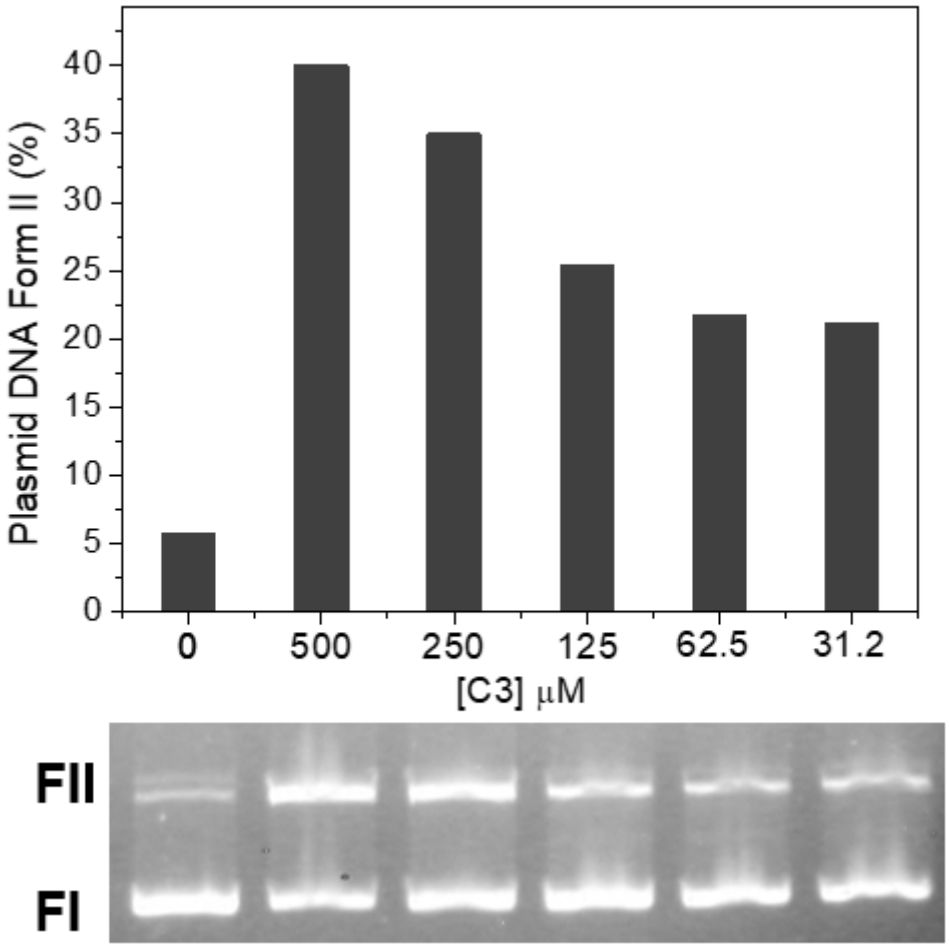

Fig. S54 Complex **C3** concentration effect on plasmid DNA cleavage. Experimental conditions: [DNA] = 330 ng, ~25 μM; [Buffer] = 10 mM, HEPES (pH 7.0); Complex concentration = 500 - 0 μM; Temperature = 50 °C; Incubation time = 8 hours sheltered from light.

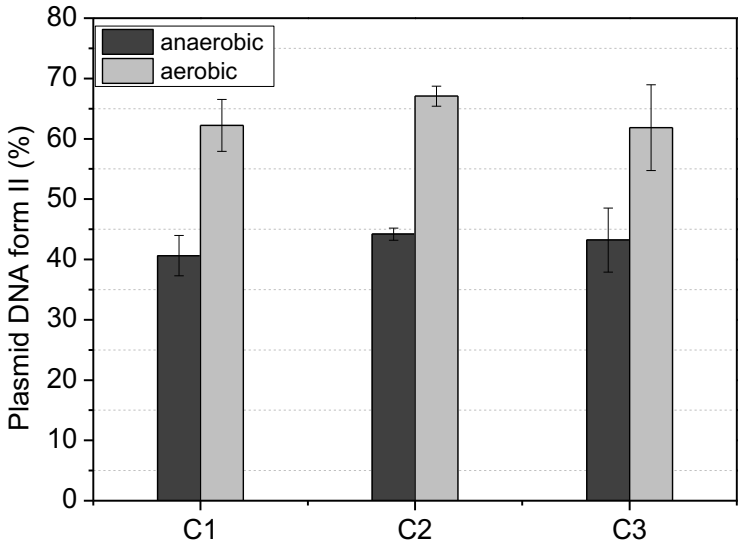

Fig. S55 Inert atmosphere effect on plasmid DNA cleavage, for complex **C1**–**C3**. Experimental conditions: [DNA] = 330 ng, ~25 μM; [Buffer] = 10 mM, HEPES (pH 7.0); Complex concentration = 500 mM; Temperature = 50 °C; Incubation time = 16 hours sheltered from light.

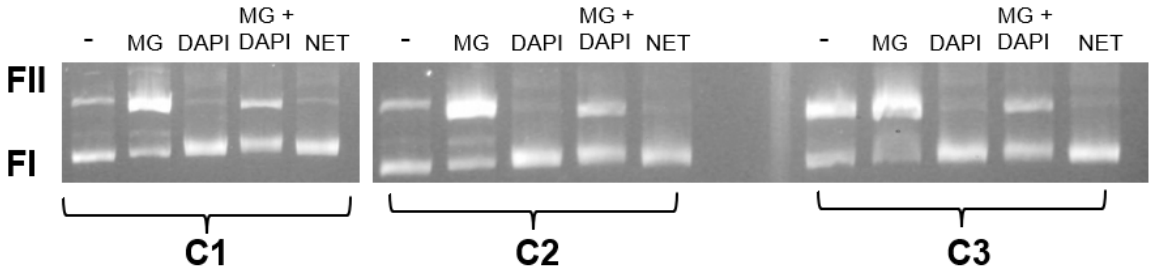

Fig. S56 Groove blockers effect on plasmid DNA cleavage, for complex **C1**–**C3**. Experimental conditions: [DNA] = 330 ng, ~25 μM; [Buffer] = 10 mM, HEPES (pH 7.0); Complex concentration = 500 μM; Temperature = 50 °C; Incubation time = 16 hours sheltered from light. [NET]=[MG]=[DAPI]= 50 μM

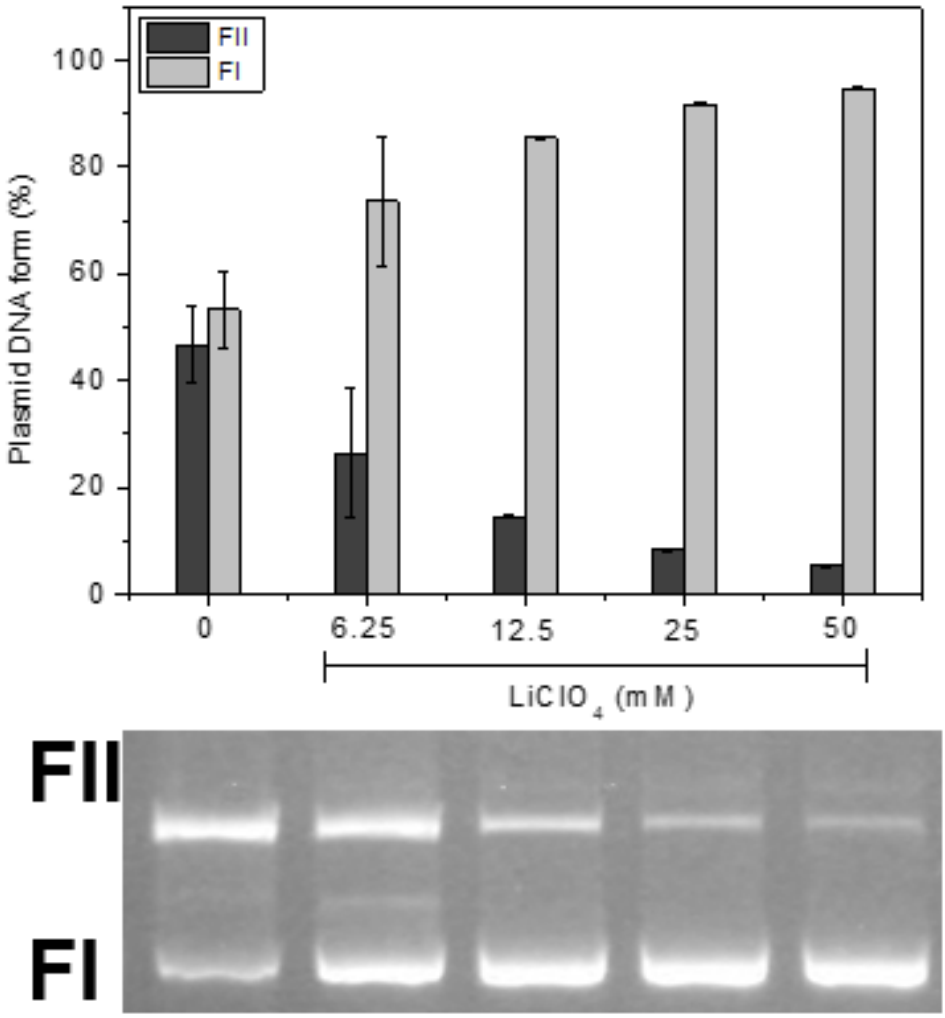

Fig. S57 Ionic strength effect on plasmid DNA cleavage, for complex **C2**. Experimental conditions: [DNA] = 330 ng, ~25 µM; [Buffer] = 10 mM, HEPES (pH 7.0); Complex concentration = 500 mM; Temperature = 50 °C; Incubation time = 16 hours sheltered from light.

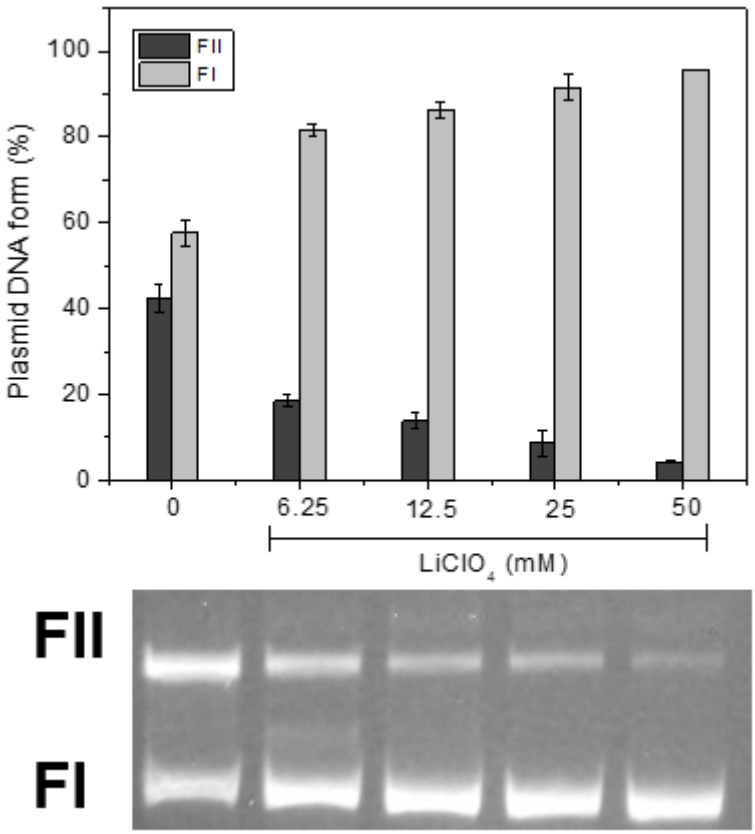

Fig. S58 Ionic strength effect on plasmid DNA cleavage, for complex **C3**. Experimental conditions: [DNA] = 330 ng, ~25 µM; [Buffer] = 10 mM, HEPES (pH 7.0); Complex concentration = 500 mM; Temperature = 50 °C; Incubation time = 16 hours sheltered from light.

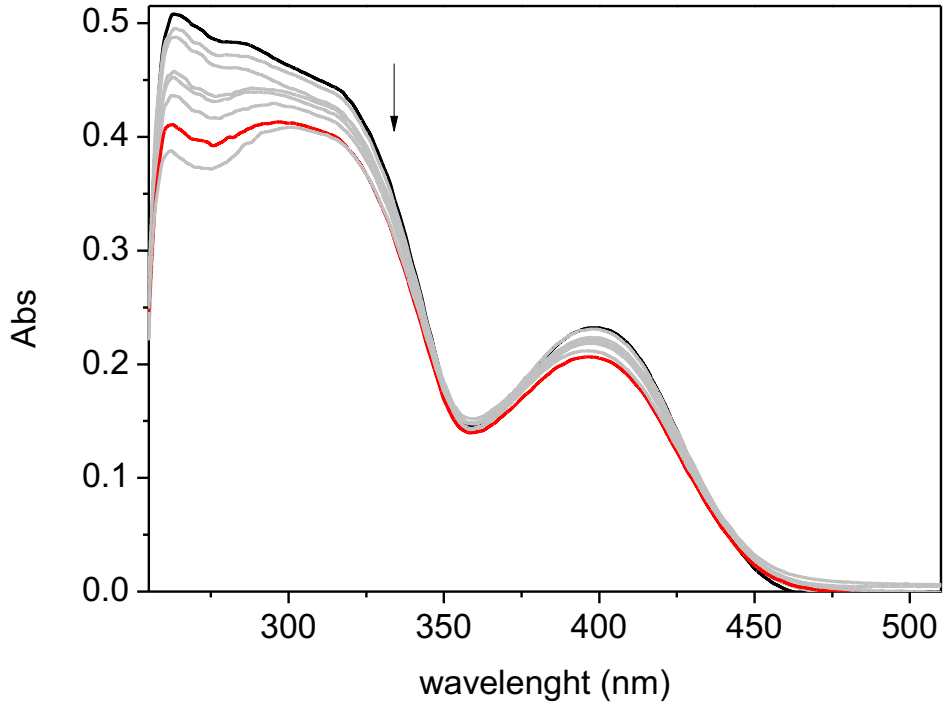

Fig. S59 Absorption spectra of complex **C1** on titration of 0–80 µM *ct*-DNA in DMF/buffer (TRIS 0.5 mM) 5% v/v; pH 7.40, *I* = 0.5 mM (NaCl); 25 °C. Arrows indicate the changes in absorbance with increasing concentration of CT-DNA.

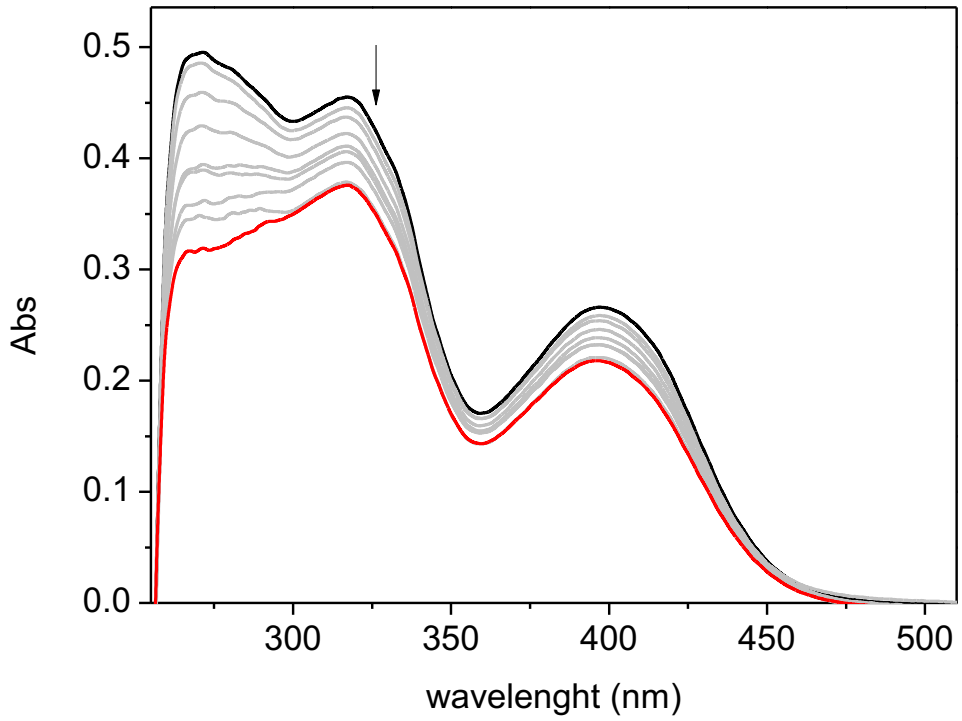

Fig. S60 Absorption spectra of complex **C2** on titration of 0–80 µM ct-DNA in DMF/buffer (TRIS 0.5 mM) 5% v/v; pH 7.40, *I* = 0.5 mM (NaCl); 25 °C. Arrows indicate the changes in absorbance with increasing concentration of CT-DNA.

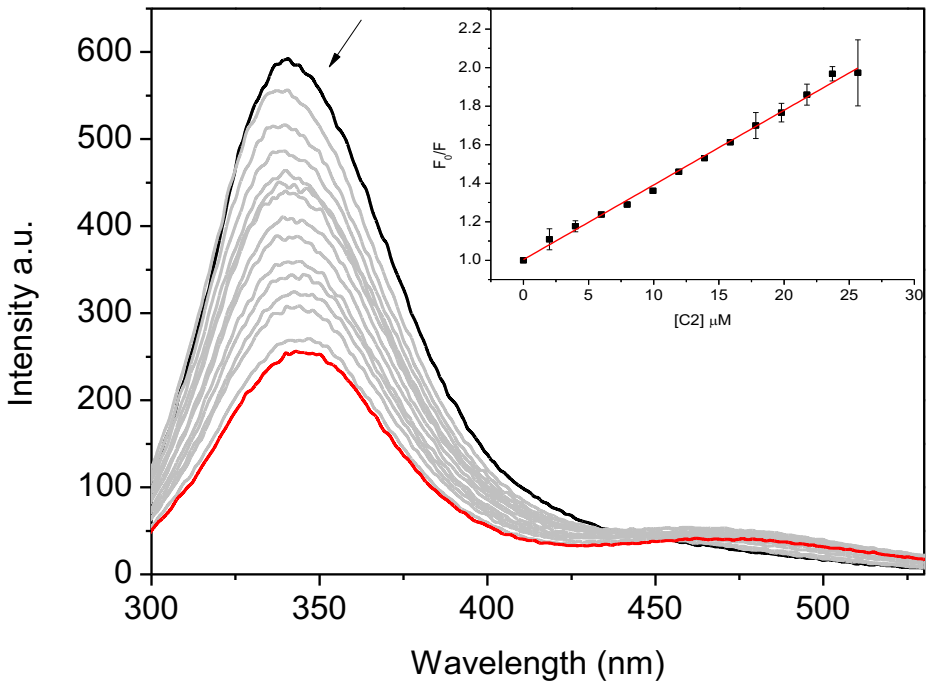

Fig. S61 Fluorescence spectrum of BSA (2 μM) quenched by complex **C2** in the concentration range of 0–20 μM. Inset: the Stern–Volmer plot.

Electronic Supplementary Information references

1 F. M. Martins, B. A. Iglesias, O. A. Chaves, J. L. Gutknecht Da Silva, D. B. R. Leal and D. F. Back, *Dalton Trans.*, 2024, **53**, 8315.

2 N. Kosari and F. Khamesipour, *BioMed Res. Int.*, 2022, **2022**, 1.

3 R. S. Meinel, A. D. C. Almeida, P. H. F. Stroppa, N. Glanzmann, E. S. Coimbra and A. D. Da Silva, *Chem.-Biol. Interact.*, 2020, **315**, 108850.

4 C. Fernandes, P. Chrystal, A. Pereira, A. Colli, L. Stenico, A. Ribeiro, I. Squarisi, A. Candido, D. Tavares, L. Magalhães, A. Crotti, C. Martins and M. Miranda, *Quím. Nova*, 2021, **44**, 570.

5 S. D. Kurbah, M. Asthana, I. Syiemlieh, A. A. Lywait, M. Longchar and R. A. Lal, *J. Organomet. Chem.*, 2018, **876**, 10.

6 M. Mohanty, S. K. Maurya, A. Banerjee, S. A. Patra, M. R. Maurya, A. Crochet, K. Brzezinski and R. Dinda, *New J. Chem.*, 2019, **43**, 17680.

7 A. W. Addison, T. N. Rao, J. Reedijk, J. Van Rijn and G. C. Verschoor, *J. Chem. Soc., Dalton Trans.*, 1984, 1349.